博士論文

Leukemia-associated mutations of DNMT3A inhibit differentiation of hematopoietic stem cells and promote leukemic transformation through aberrant recruitment of Polycomb repressive complex 1.

(DNMT3A変異はポリコーム抑制複合体1との異常な協調関係を通して造血幹細胞の分化阻害および白血病性形質転換の促進をもたらす。)

古屋　淳史

Contents

Summary

The impact of DNMT3A mutations in acute myeloid leukemia (AML) has been further emphasized by the recent progress in whole genome sequencing and over 20% of cytogenetically normal AML patients have somatic DNMT3A mutations with R882 being a hot spot of mutation. The precise molecular mechanisms of mutated DNMT3A in leukemogenesis are largely unknown, even though it is known that Dnmt3a controls the epigenetic silencing of hematopoietic stem cell (HSC) regulatory genes through loss-of-function study. Here I show that, in murine transplantation experiments, recipients transplanted with DNMT3A mutant-transduced cells exhibit HSC accumulation. Differentiation-associated genes such as PU.1 are down-regulated without accompanying changes in methylation status of their promoter-associated CpG islands in DNMT3A mutant-transduced stem/progenitor cells, indicative of DNA methylation-independent mechanism. DNMT3A R882 mutant also promotes monoblastic transformation of murine bone marrow cells in vitro in combination with HOXA9 and contributes to insensitivity to ATRA-induced differentiation in AML cells. Molecularly, DNMT3A R882 mutant interacts with polycomb repressive complex 1

(PRC1), leading to transcriptional silencing of PU.1. Suppression of the PRC1 complex impairs aberrant HSC accumulation, monoblastic transformation, and ATRA insensitivity by DNMT3A R882 mutation. Taken together, my results highlight the functional role of DNMT3A mutation, forming the basis for leukemia development.

Introduction

Given that acute myeloid leukemia (AML) is a molecularly heterogeneous group of malignancies, each AML subtype is diagnosed based on multiple laboratory tests including cytogenetics and FISH. The classical taxonomy French-American-British (FAB) classification has contributed greatly to AML diagnosis mainly by morphology of leukemia cells. However, on the arrival of next generation sequencing, the genetic landscape of AML is going to be totally unveiled, leading to the need for the refined categorization of AML based on multiple profiles. For instance, among cytogenetically normal AML (CN-AML), NPM1-mutated AML or CEBPα-mutated AML compose an original disease entity, which is reflected on the 2008 revision of the World Health Organization classification, in which karyotype abnormalities, morphology, and some frequent genetic features are key determinants[1]. The recent detailed mutational analyses have revealed several gene mutations in CN-AML, including DNMT3A, TET2, IDH1/2, and ASXL1[2-5]. Especially in these mutations, somatic mutations of DNMT3A, a member of DNA methyltransferases, occur in about 20% of AML, are mostly heterozygous and more frequently associated with CN-AML[6-8]. The characteristics of DNMT3A-mutated AML are the recurrence (30-35%) and the poor overall survival[7-10].

DNMT3A mutations closely associate with NPM1, FLT3 and IDH1 mutations and frequently found in FAB M4/M5 myelomonocytic/monocytic AML[7,8,11]. Molecularly, DNA methyltransferases catalyze the transfer of a methyl group to the cytosine of CpG dinucleotides and, in particular, DNMT3A and DNMT3B are the main enzymes involved in de novo methylation, and their deficiency deprives embryonic stem cells (ESCs) of differentiation potential[12]. R882 is the hot spot to be mutated in AML, where R882H is the most prevalent, accounting for about 70-80% cases and R882C is the second most. It has recently reported that DNMT3A mutations caused loss of tetramerization capacity in vitro which led to defective methylase activity[6,8,13]. Although the most recent landmark analysis has revealed that DNMT3A-mutated AML samples have an apparent DNA hypo-methylation signature, there are no distinct gene expression profiles regarding DNMT3A mutations[11]. In conditional Dnmt3a-knockout mice studies, Dnmt3a-deleted hematopoietic stem cells (HSCs) have reduced differentiation potential leading to marked expansion of HSCs in vivo and up-regulation of self-renewal genes, which implied a critical role of Dnmt3a wild-type (WT) in silencing self-renewal of HSCs and in allowing for hematopoietic differentiation[14,15]. Although Dnmt3a loss causes both hypo- and hyper-methylation of HSCs in mice, some of HSC-associated genes such as Runx1 and Gata3 have hypo-methylated regions with

accompanying up-regulation of these genes, consistent with the classic regulatory model[14].

Polycomb-group proteins (PcG), global epigenetic transcriptional repressors, play crucial roles in many biological processes, including stem cell self-renewal, differentiation, and cancer development[16]. PcG proteins reside in two major complexes, polycomb repressive complex 1 (PRC1) and PRC2. PRC2 complex catalyzes lysine 27 tri-methylation on histone H3 (H3K27me3), initiating gene suppression[17,18]. One currently and widely accepted hierarchical model is that CBX proteins in PRC1 complex recognize H3K27me3 and bind to these loci, followed by recruitment of PRC1 complex for the maintenance of gene silencing via chromatin compaction and placement of a repressive mark, histone H2AK119 ubiquitination[19,20]. In hematological malignancy development, as previously reported, the recruitment of PRC2 complex by PML/RARα fusion protein to retinoic acid (RA)-responsive genes is a critical step in the development of acute promyelocytic leukemia (APL)[21], and PLZF/RARα fusion protein which exhibits more severe phenotype of APL interacts with not only PRC2 complex but also PRC1 complex, accounting for non-response to all-trans RA treatment[22]. More recently, several groups have elucidated that Ezh2, a component of

PRC2 complex, is required for maintenance of MLL-AF9-mediated mouse leukemia model[23,24].

DNMT3A is well known to interact with several histone modifiers including PcG proteins to suppress their target gene expression[25-29]. The functional cooperation between DNA methyltranferase and PcG proteins is considered to be responsible for cancer development[30,31]. Indeed, 50% of genes frequently hyper-methylated in colon or prostate cancer are marked by H3K27me3 for de novo DNA methylation, consistent with the fact that EZH2 directly interacts with DNMT1, DNMT3A, and DNMT3B[25,32]. Similarly, CBX proteins and BMI1, components of PRC1 complex, also interacts with DNA metyltransferases and DNMT-associated protein DMAP1, respectively[26,33].

In spite of the recent progress listed above in DNMT3A studies, the mechanism through which DNMT3A mutations contribute to AML remains elusive. To clarify the function of DNMT3A mutation in leukemogenesis, I describe the characterization of exogenous DNMT3A R882 mutants in the hematopoietic compartment, elucidating that DNMT3A R882 mutant exhibits differentiation block of HSCs and promotes monoblastic transformation, in collaboration with HOXA9. Furthermore, I show that the enhanced interaction between DNMT3A R882 mutants and PRC1 complex leads to aberrant recruitment of PRC1 complex to regulatory regions of hematopoietic

differentiation-associated genes. These findings provide new insights into how DNMT3A mutation contributes to malignant transformation.

Materials and Methods

Plasmids

Plasmids encoding proteins of human wild-type DNMT3A, Flag- and Myc-tagged DNMT3A and its mutants cDNA were cloned into the EcoR1/BamH1 site of pBleuscript II. R882H and R882C mutants were constructed from wild-type DNMT3A by means of a PCR method. To produce protein expressing retrovirus and lentivirus, I used the following plasmids: pGCDNsam-DNMT3A WT-, R882H-, and R882C-IRES-EGFP, pGCDNsam-DNMT3A WT-, R882H-, and R882C-IRES-Kusabira Orange (KuOr), CSII-EF-DNMT3A WT-, R882H-IRES2-Venus, CSIV-TRE-DNMT3A WT-, R882H-UbC-KT, pMYs-FLT3-ITD-IG, pMYs-HOXA9-IG, and pMYs-PU.1-IG. All of the PCR products were verified by DNA sequencing. The other plasmids used for transfection were as follows; pcDNA3-Flag-DNMT3A WT, R882H, and R882C, pcDNA3-Flag-BMI1, and pcDNA3-Flag-RING1B.

Mice

Heterozygous Bmi1 knockout (KO) mice ($Bmi1^{+/-}$ mice) were previously described[34]. Littermates were used as controls in all experiments. All animal experiments were approved by The University of Tokyo Ethics Committee for Animal Experiments and strictly adhered to the guidelines for animal experiments of The University of Tokyo. $Bmi1^{+/-}$ mice were genotyped by PCR as follows: Genomic DNA was isolated from tail biopsies and subjected to PCR using the primers to detect WT and KO allele. The PCR samples were denatured at 94°C for 3 min, subjected to 30 cycles of amplification (94°C for 45 s, 65°C for 45 s, and 72°C for 45 s for WT allele, and 94°C for 45 s, 58°C for 45 s, and 72°C for 45 s for KO allele), and followed by a final extension step at 72°C. PCR products were resolved by agarose gel electrophoresis. PCR primers are listed below: WT forward, AGCAGCAATGACTGTGATGC, and reverse, GTTGCTGGTTCCATTCATGG; KO forward, TCGTTATGTTTATCGGCACTTT, and reverse, AACATCGCCTCGCTCCAGTCAA.

Cell Culture

Human embryonic kidney (HEK) 293T cells were grown in D-MEM with 10% fetal calf serum (FCS) and 1% penicillin and streptomycin (PS) at 37°C in a 5% CO_2 incubator. HL-60, KG-1, and THP-1 cells were grown in RPMI1640 with 10% FCS and

1% PS at 37°C in a 5% CO_2 incubator. OCI-AML3 cells were grown in α-MEM with 20% FCS and 1% PS at 37°C in a 5% CO_2 incubator. KG-1 cells were provided by the RIKEN BRC through the National Bio-Resource Project of the NEXT, Japan. OCI-AML3 cells were provided by the German Resource Centre for Biological Material (DSMZ, Germany). For ATRA stimulation, cells were treated with 1 μM ATRA for the indicated time.

Retrovirus Production and Bone Marrow Transplantation (BMT) Assays

To obtain retrovirus supernatants, Plat-E packaging cells were transiently transfected with retroviral constructs. 5-fluorouracil (5-FU)-primed or c-kit+-sorted C57/B6 mouse bone marrow (BM) cells were purified and incubated in α-MEM with 20% FCS, 1% PS, and cytokines (50 ng/mL mouse SCF and 25 ng/mL human TPO, IL-6, and FLT3) at 37°C in a 5% CO_2 incubator for 24 h. Subsequently, cultured cells were infected with retrovirus in the presence of RetroNectin (Takara Bio Inc.). The infected cells were harvested 48 h after retrovirus infection, and vector-transduced cells were sorted and subjected to in vitro culture and in vivo transplantation assay. These cells were injected into lethally irradiated (9.5 Gy) recipient mice. For experiments of assessing the repopulating capacity, 5-FU-primed mouse BM cells were transduced with

pGCDNsam-EGFP, pGCDNsam-DNMT3A WT-IRES-EGFP, pGCDNsam-DNMT3A R882H-IRES-EGFP, or pGCDNsam-DNMT3A R882C-IRES-EGFP, and 3×10^4 GFP+ cells were transplanted with 2×10^5 unfractionated competitor BM cells from congenic mice. For assessing the repopulating capacity on Bmi1 heterozygosity, c-kit+ $Bmi1^{+/+}$ or $Bmi1^{+/-}$ mouse BM cells were transduced with same vectors, and 2×10^5 GFP+ cells were transplanted with the same number of unfractionated competitor BM cells from congenic mice. For second BMT assays, c-kit+ BM cells were obtained from recipient mice transplanted the cells transduced with pGCDNsam-IRES-KuOr, pGCDNsam-DNMT3A WT-IRES- KuOr, or pGCDNsam-DNMT3A R882H-IRES-KuOr four weeks after transplantation. Then, these cells were transduced with pMYs-IG or pMYs-PU.1-IG, and 2×10^5 GFP and KuOr double positive cells were transplanted with 1×10^5 unfractionated competitor BM cells from congenic mice to lethally irradiated mice.

Flow Cytometry and Cell Cycle Analysis

A list of antibodies is provided in Table 1. Stained cells were sorted with a FACSAriaII (BD), and analysis was performed on LSRII (BD). A mixture of antibodies recognizing CD3, CD4, CD8, B220, CD127, TER-119, Mac-1, or Gr-1 was used to

identify Lin+ cells. The data analyses were performed with FlowJo software (Tree Star). For the cell cycle analysis, after LSK staining, bone marrow cells were fixed and permeabilized using BD Cytofix/Cytoperm Fixation/Permeabilization Solution Kit (BD Biosciences) according to the manufacturer's recommendations. Subsequently, I stained with DAPI (Molecular Probes) and PE Ki-67 (BD Biosciences).

Real-Time Quantitative PCR (qPCR)

Real-time quantitative PCR was carried out on the LightCycler480 system (Roche) using SYBR Green reagents according to the manufacturer's instructions. The results were normalized to 18s rRNA levels. Relative expression levels were calculated using the $2\text{-}\Delta\Delta C_T$ method. A list of primers is provided in Table 2.

Targeted Bisulfite Sequencing

Genomic DNA samples were extracted from GFP+LSK cells of transplanted mice and were subjected to bisulfite conversion with the EpiTect bisulfite kit (Qiagen) according to the manufacturer's instructions. Bisulfite-treated DNA was amplified with by PCR using gene-specific primers. PCR products were cloned into the pTAC2 vector (BioDynamics Laboratory), transformed into competent bacteria and sequenced.

Visualization of bisulfite sequence data for CpG methylation was performed using the QUMA web-based tool[35]. Sequences for the primers used in this study are provided in Table 2.

Lentivirus Production and Transduction of AML Cell Lines

To obtain lentivirus supernatants, HEK293T cells were transiently transfected with lentiviral vectors, MD2G packaging plasmid (Invitrogen), and PAX2 envelope plasmid (Invitrogen). The viral supernatant was collected 48 h after transfection and filtered to remove cellular debris. AML cell lines were infected with lentivirus in the presence of RetroNectin (Takara Bio Inc.). The infected cells were harvested 72 h after retrovirus infection, and vector-transduced cells were sorted and subjected to in vitro culture. When we used CSIV-TRE-RfA-UbC-KT doxycycline-inducible lentiviral vector, 1 μg/mL DOX was added to induce transgene expression.

siRNA Interference

Specific shRNAs targeting human RING1B mRNAs were designed and cloned into pSIREN-RetroQ-ZsGreen vector. Control shRNA is a nonfunctional construct provided from Clontech. The target sequences, from 5’ to 3’, were

GGAACTCAACCATTAAGCA (shRING1B #1), GGACTGCAATTATTCAGTA (shRING1B #2). To obtain amphotropic retrovirus supernatants, Plat-A packaging cells were transiently transfected with these constructs. Cultured cells were infected with amphotropic retrovirus in the presence of RetroNectin (Takara Bio Inc.). The infected cells were harvested 72 h after amphotropic retrovirus infection, and vector-transduced cells were sorted and subjected to in vitro culture.

Assessment of Total CpG Methylation

Total DNA methylation was measured as previously described[36]. In brief, 1×10^5 cells were washed with PBS, and fixed and permeabilized using BD Cytofix/Cytoperm Fixation/Permeabilization Solution Kit (BD Biosciences) according to the manufacturer's recommendations. Cells were incubated with anti-5-methylcytosine antibody (Calbiochem, NA 81) at 1:100 dilution for 30 min at room temperature. After washing with PBS, cells were incubated with secondary antibody coupled with Alexa Fluor 700 (Invitrogen) for 30 min in a dark-room environment.

Immunoprecipitation and Western Blotting

Cell lysates were incubated with each antibody for 2 h at 4°C. Then, the samples were incubated with protein G–Sepharose (Amersham) for 1 h at 4°C. The precipitates were washed twice with the TNE buffer, twice with high salt-containing wash buffer (50 mM Tris-HCL [pH7.5], 500 mM NaCl, 0.1% Nonidet P40 (NP-40), 0.05% sodium deoxycholate), and once with low salt containing buffer (50 mM Tris-HCL [pH7.5], 0.1% NP-40, 0.05% sodium deoxycholate) for epitope-tagged proteins, or washed five times with the TNF buffer for endogenous proteins. Then, the precipitates were analyzed by Western blotting. Blots were detected using an ImmunoStar Zeta (Wako Pure Chemical Industries) and an LAS-3000 image analyzer (Fujifilm) as recommended by the manufacturers. Immunoprecipitation and western blotting were performed using anti–Flag (Sigma-Aldrich), anti-Myc (Cell Signaling), anti-DNMT3A (Santa Cruz), anti-BMI1 (Millipore), anti-MEL18 (Santa Cruz), anti-RING1B (Cell Signaling), anti-RYBP (Millipore), anti-CBX7 (Abcam), and anti-β-actin (Cell Signaling) antibodies.

Colony-Forming Assays and Cell Proliferation Analysis

In each experiment, cells were plated into Methocult3434 (StemCell Technologies) medium. Colony numbers of each dish were scored on day 7. The number of cells

seeded into the plate was described in each figure legend. HOXA9-transduced immortalized cells after fourth round were then transferred into liquid cultute (RPMI1640 with 10% FCS, 10% conditioned medium from the WEHI-3B cell line, and 1% PS at 37°C in a 5% CO_2 incubator for cell proliferation analysis.Immortalized cells were cytospun and stained with Wright-Giemsa.

ChIP and Quantitative PCR

Cells were crosslinked with 1% of formaldehyde at room temperature for 15 min, and the reaction was stopped by the addition of glycine (2.5 M). Cells were rinsed three times with cold PBS, resuspended in lysis buffer 1 (50 mM HEPES-KOH [pH 7.5], 140 mM NaCl, 1 mM EDTA, 10% Glycerol, 0.5% NP-40, 0.25% Triton, Roche protease inhibitor cocktail (Roche), and 1 mM PMSF) and rocked at 4°C on platform rocker for 10 min. After centrifugation, each pellet was resuspended in lysis buffer 2 (10 mM Tris-HCl [pH 8.0], 200 mM NaCl, 1 mM EDTA, 0.5 mM EGTA, Roche protease inhibitor cocktail (Roche), and 1 mM PMSF) and rocked at room temperature for 10 min. After centrifugation, each pellet was resuspended in lysis buffer 3 (10 mM Tris-HCl [pH 8.0], 100 mM NaCl, 1 mM EDTA, 0.5 mM EGTA, 0.1% sodium-deoxycholate, 0.5% N-lauroylsarcosine, Roche protease inhibitor cocktail

[Roche], and 1 mM PMSF) and sonicated with a ultrasonication (Covaris). Lysates were diluted with buffer 3 containing 1% TRITON X-100. When I utilized MNase, cell pellet was resuspended in MNase buffer (10 mM NaCl, 50 mM Tris [pH 7.5], 2.5 mM MgCl2, 0.1% NP-40, 1mM DTT, EDTA free protease inhibitor cocktail, 10 mM CaCl2), and subjected to MNase digestion with 10000 U/mL (New England Biolabs). The digestion was stopped by adding EDTA and diluted with buffer-L (20 mM Tris-HCl [pH 7.5], 150 mM NaCl, 0.5 mM EGTA, 1% Triton X-100, 0.1% sodium-deoxycholate, 0.1% SDS, and protease inhibitor cocktail), followed by ultrasonication. Then, 40 μL of Dynabeads Protein G (Invitrogen) preloaded with 2 μg of each antibody were added to the lysates for 2 h and then stringently washed for 5 times with wash buffer (50mM HEPES-KOH [pH7.5], 500 mM LiCl, 1 mM EDTA, 1% NP-40, and 0.7% sodium deoxycholate). Bound DNA fragments were eluted and quantified by subsequent real-time PCR. The antibodies used in ChIP assays were as follows: anti-Flag (Sigma-Aldorich), anti-DNMT3A (Abcam), anti-BMI1 (Millipore), anti-RING1B (Cell Signaling), anti-uH2A (Cell Signaling). A list of primers is provided in Table 2.

Statistical Analysis

Statistical significance of differences between different groups was assessed with a 2-tailed unpaired t test. Differences were considered statistically significant at a p value of less than 0.05.

Results

DNMT3A R882 mutation endows human AML cell lines with resistance to ATRA-induced neutrophil differentiation.

I first investigated whether DNMT3A WT and R882 mutant could affect proliferation of human AML cell lines. I lentivirally transduced empty vector (EV), WT, or R882H to HL-60 and KG-1 cell lines which did not carry DNMT3A mutation[37]. DNMT3A WT-transduced AML cell lines resulted in decreased proliferation relative to EV and R882H-transduced cells (Figure 1).

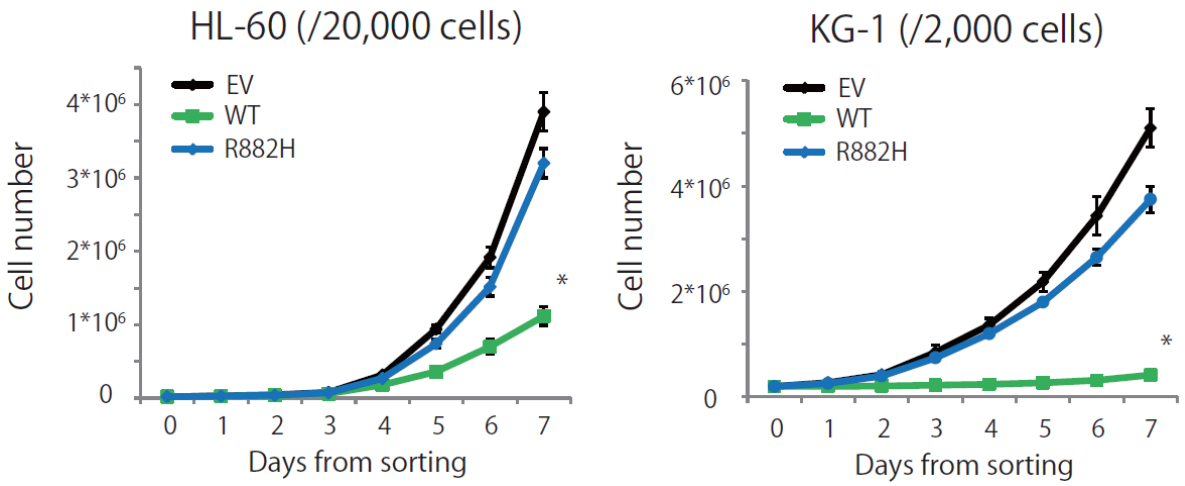

Figure 1. Growth curve of HL-60 (Left) and KG-1 (Right) cells transduced with EV, DNMT3A WT, or DNMT3A R882H. (N = 3 replicate experiments) Data are mean±SD values. *p<0.05

Subsequently, I evaluated the morphology of these transduced cells. DNMT3A WT-transduced HL-60 cells had some features of mature myeloid cells, such as small cell size, reduced nucleus-to-cytoplasm ratio, and segmented nucleus, whereas DNMT3A mutant-transduced cells remained immature morphology (Figure 2).

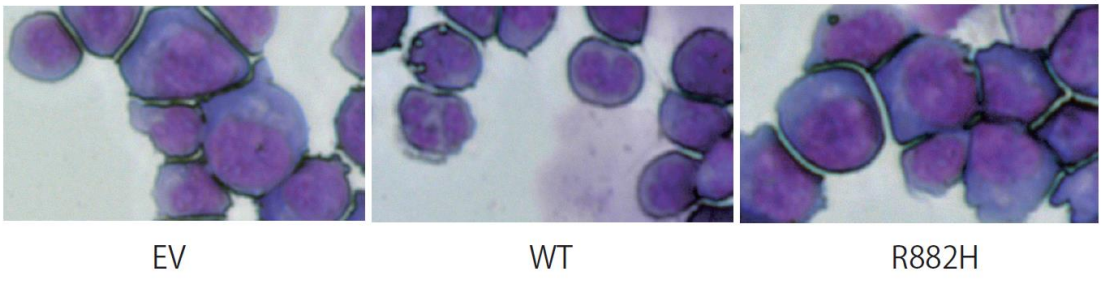

Figure 2. Typical morphology of HL-60 cells transduced with EV, DNMT3A WT, or DNMT3A R882H.

Next I quantified the levels of CD11b (Mac-1), a marker of myeloid lineage, of these cells five days and 10 days after transduction by flow cytometry. HL-60 cells did not express CD11b under normal condition and induction of differentiation by ATRA induced CD11b expression. CD11b positive rate was increased by more than 10-fold in DNMT3A WT-transduced cells compared to EV and R882H-transuduced cells (Figure 3A and 3B). These morphologic and surface marker analyses demonstrated that

DNMT3A WT promote differentiation of AML cell lines whereas R882H mutant is defective in induction of differentiation.

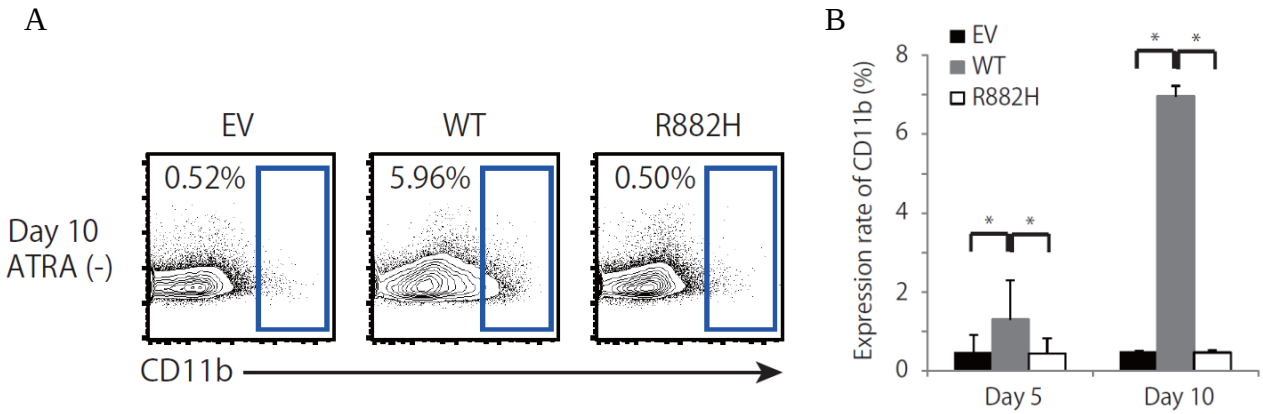

Figure 3. (A) Representative surface marker CD11b expression analyzed by flow cytometry of HL-60 cells transduced with EV, DNMT3A WT, or DNMT3A R882H. The boxed region shows CD11b positive rate at 10 days after transduction with EV, DNMT3A WT, or DNMT3A R882H. (B) Cumulative data of CD11b positive rate at five and 10 days after transduction with EV, DNMT3A WT, or DNMT3A R882H in HL-60. (N = 3 replicate experiments) Data are mean ± SD values. *p<0.05

Additionally, there showed a marked difference in differentiation capacity induced by ATRA between DNMT3A WT-transduced HL-60 cells and R882H-transduced HL-60 cells (Figure 4A and 4B).

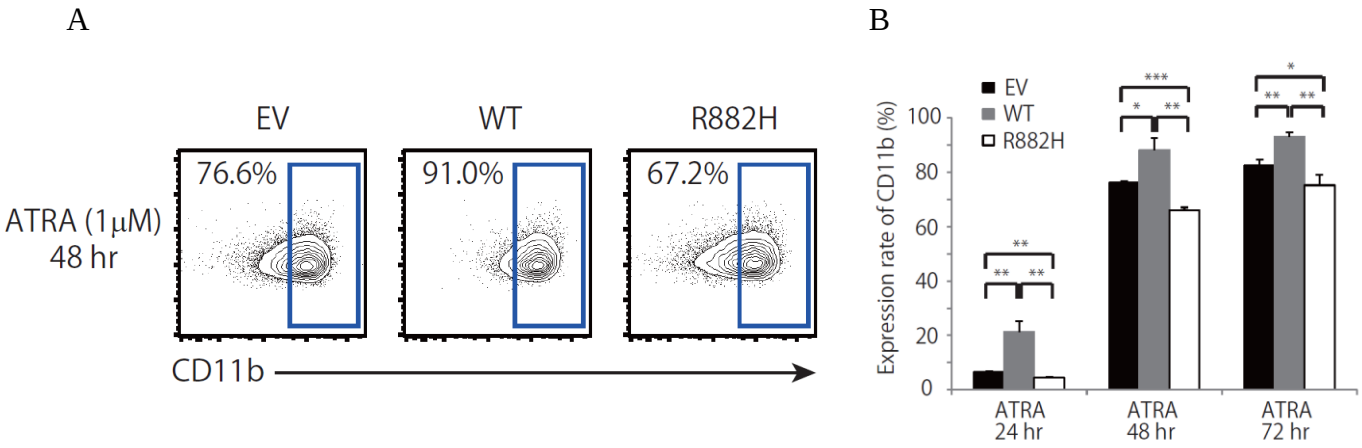

Figure 4. (A) Representative surface marker CD11b expression analyzed by flow cytometry of HL-60 cells transduced with EV, DNMT3A WT, or DNMT3A R882H. The boxed region shows CD11b positive rate at 48 h after transduction and administration of ATRA (1μM). (B) Cumulative data of CD11b positive rate 24, 48, and 72 h after transduction with each vectors and administration of ATRA (1μM). (N = 3 replicate experiments) Data are mean±SD values. *p<0.05, **p<0.01, ***p<0.001

Taken together, these results indicate that DNMT3A WT induces terminal myeloid differentiation and inhibits proliferation of human AML cell lines, whereas R882 mutant produces resistance to ATRA-induced neutrophil differentiation.

DNMT3A R882 mutation causes hematopoietic stem cell accumulation.

I next investigated the effects of exogenous expression of DNMT3A R882 mutant protein in hematopoiesis by transducing 5-FU-primed mouse bone marrow cells with retroviral EV-, DNMT3A WT-, R882H-, or R882C-IRES-EGFP. GFP+ cells were sorted, then plated in methylcellulose to evaluate the colony-forming capacity in vitro and transplanted to lethally irradiated mice for assessing the repopulating capacity in vivo (Figure 5).

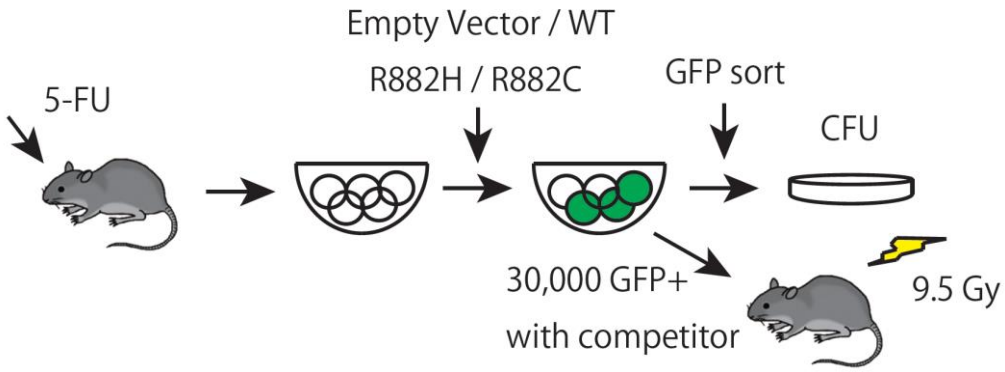

Figure 5. Design of colony-forming assay and competitive repopulating assay with EV-, DNMT3A WT-, or DNMT3A R882 mutant-transduced 5-FU-primed murine BM cells.

DNMT3A mutant-transduced cells generated comparable hematopoietic colonies to those of EV-transduced cells, while DNMT3A WT-transduced cells had a reduced

colony-forming capacity on the first round. All four types of cells could be replated up to the fourth round, which showed no sign of immortalization in vitro (Figure 6).

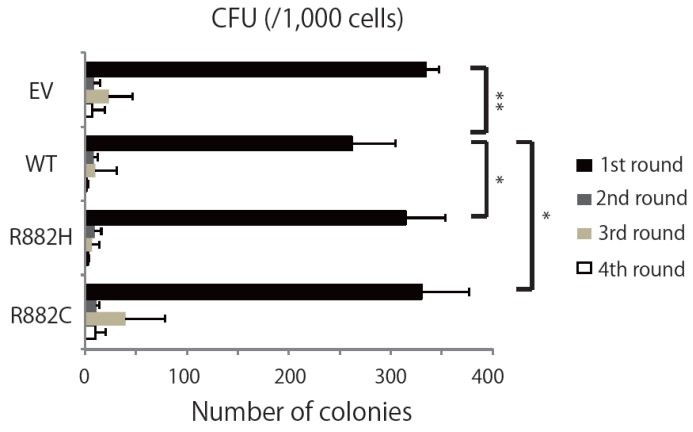

Figure 6. Cumulative colony-forming capacity of each 1000 transgene-expressing cells at the initial plating is shown. (N = 5 replicate plates). Data are mean±SD values. *p<0.05, **p<0.01

In murine BMT experiments, recipients transplanted with WT-transduced cells consistently exhibited lower chimerism in peripheral blood (PB) from four weeks after transplantation compared to EV control mice. On the other hand, recipients transplanted with R882 mutant-transduced cells showed comparable PB chimerism to EV-control (Figure 7A). Moreover, DNMT3A R882 mutant-transduced HSCs retained multilineage differentiation capacity up to 16 weeks after BMT compared to DNMT3A WT-transduced HSCs (Figure 7B).

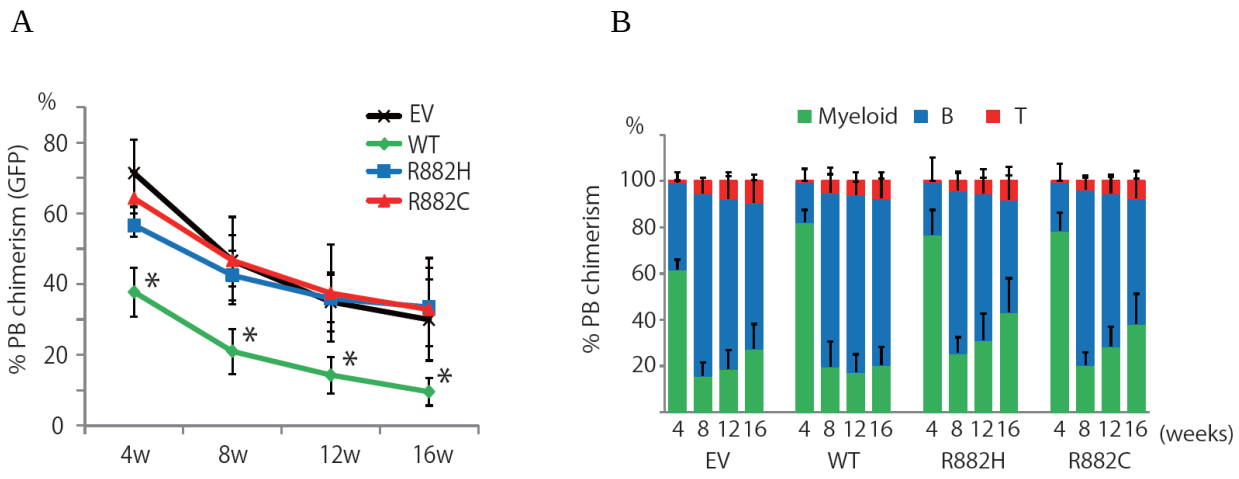

Figure 7. (A) Contribution of EV, WT, R882H, and R882C to PB chimerism in primary competitive transplants, measured every four weeks. (N = 5-6 mice). (B) PB lineage distribution of the mice transplanted with EV-, WT-, or R882 mutant-transduced cells. Shown are percentage of donor-derived (GFP+) myeloid cells, B cells, and T cells, measured every four weeks. (N = 5-6 mice). Data are mean±SD values. *p<0.05

These mice transplanted with R882 mutant-transduced cells did not exhibit any signs of leukemia for one-year observation (Figure 8), suggesting that retroviral overexpression of DNMT3A R882 mutant alone is insufficient to induce leukemic transformation in vitro and in vivo.

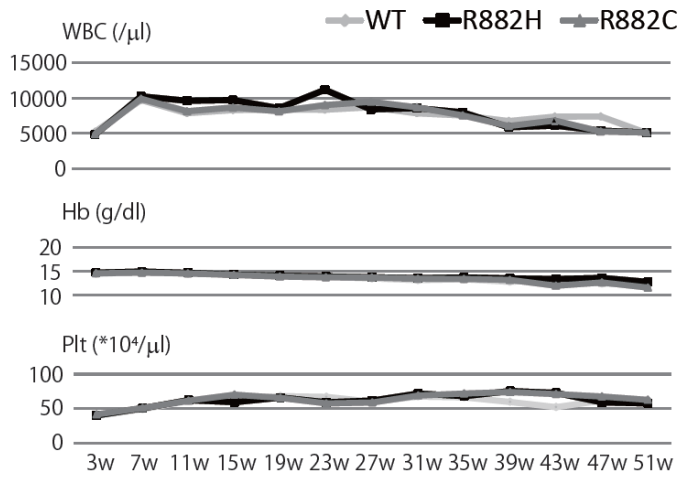

Figure 8. The plots of white blood cell count (Top), hemoglobin levels (Middle), and platelet count (Bottom) in PB up to one year after transplantation (N = 9 mice). Data are mean values.

Because DNMT3A R882 mutant-overexpressed cells showed a superior engraftment to DNMT3A WT-overexpressed cells in PB of transplants, I sacrificed these transplanted mice at four weeks post-transplant and investigated whether exogenous expression of DNMT3A WT and R882 had altered BM stem/progenitor frequencies. Interestingly, while frequency of long-term HSC (LT-HSC; lineage- (L), Sca1+ (S), c-kit+ (K), CD150+, CD48-) was decreased in recipients of DNMT3A WT-transduced cells, R882 mutant caused an increase in LT-HSC frequency compared to EV-control recipients (Figure 9A and 9B).

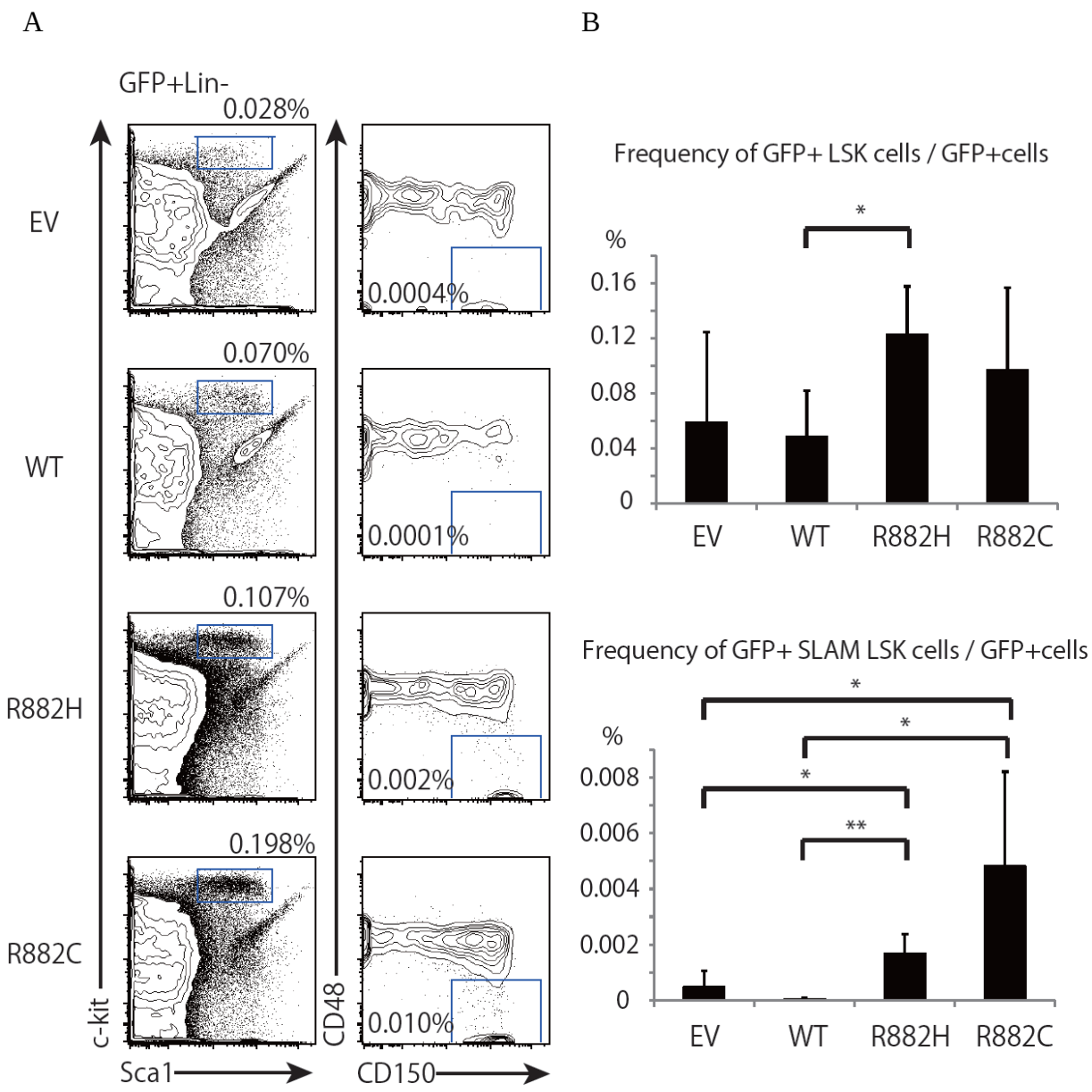

Figure 9. (A) Representative flow cytometry data of BM cells from transplanted mice. The left boxed regions show the frequency of GFP+LSK cells in GFP+ cells. The right boxed region shows the frequency of GFP+CD150+CD48-LSK cells in GFP+ cells. (B) Cumulative data of the frequency of GFP+LSK cells in GFP+ cells (Upper) and GFP+SLAM LSK cells in GFP+ cells (Lower). (N = 5-6 mice). Data are mean±SD values. *p<0.05, **p<0.01

Cell cycle analysis revealed that the percentage of cells in DAPI-Ki67- (G0 status; quiescent) was higher and the percentage of Ki67+ (proliferating) cells was lower in DNMT3A R882 mutant-transduced LSK cells compared to EV- and DNMT3A WT-transduced cells (Figure 10A and Figure 10B).

A

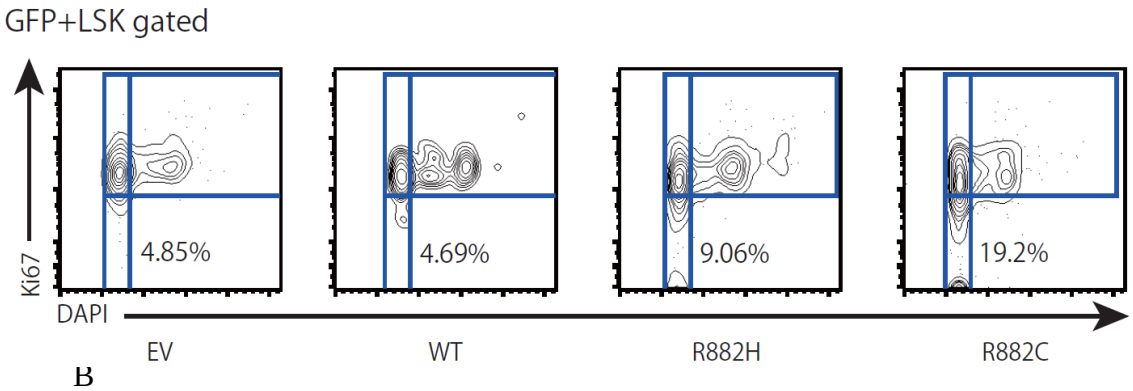

B

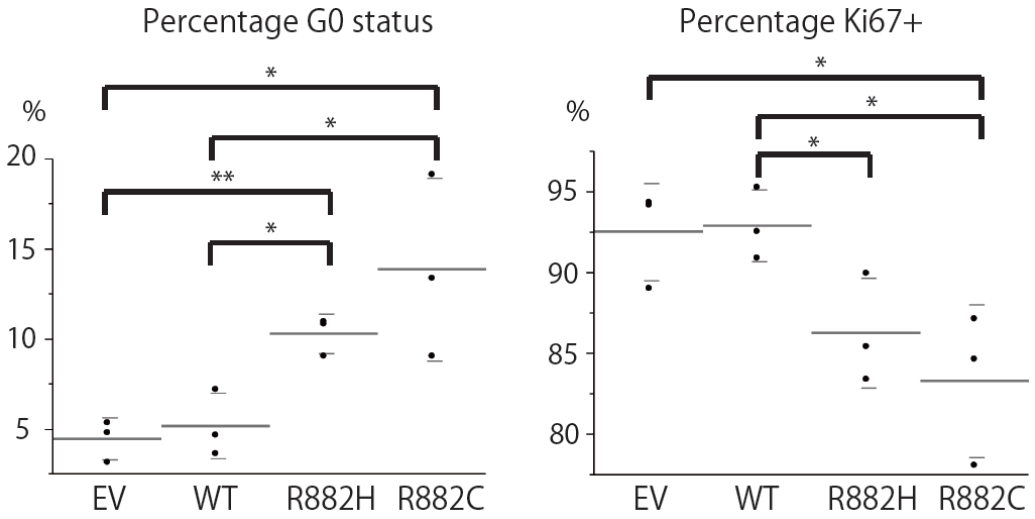

Figure 10. (A) Representative flow cytometry data of cell cycle analysis. Murine BM cells were harvested from transplanted mice four weeks post-transplant and were gated first by GFP+LSK. The left lower boxed region shows the percentage of cells in G0 status in GFP+LSK cells. (B) Dot plots of the percentage of cells in G0 status (Left) and the percentage of Ki67 positive cells (Right). (N = 3 mice). Data are mean±SD values. *p<0.05, **p<0.01

These results demonstrate that exogenous expression of DNMT3A R882 mutation contributes to accumulation of quiescent HSCs, while overexpression of DNMT3A WT reduces frequency and functional repopulating capacity of HSCs.

DNMT3A R882 mutation results in up-regulation of Hoxb cluster and down-regulation of differentiation-associated genes.

To clarify down-stream target genes of mutant DNMT3A that evoked HSC accumulation, I sorted GFP+LSK cells from transplanted mice at four weeks post-transplant and conducted quantitative PCR experiment of various hematopoiesis-related genes which were deregulated in clinical AML samples harboring DNMT3A mutations and in Dnmt3a conditional knockout mice study described previously[14]. DNMT3A R882 mutant-transduced LSK cells showed higher Hoxb2 and Hoxb4 expression, both of which are known to be highly expressed in clinical AML samples harboring DNMT3A mutation[8]. On the other hand, Hoxa9 expression which is also highly expressed in clinical AML samples was not altered (Figure 11). Conversely, myeloid differentiation-associated genes, including PU.1 and Cebpα, were down-regulated in DNMT3A mutant-transduced LSK cells. Other genes such as Nr4a2, a HSC fingerprint, Runx1 and Foxo1, both known to be essential for HSC function,

were up-regulated but not significantly in DNMT3A R882 mutant-transduced stem/progenitor cells. The trends of these gene expressions in DNMT3A R882 mutant-transduced stem/progenitor cells were similar to those of Dnmt3a-null HSCs as described previously[14] (Figure 11).

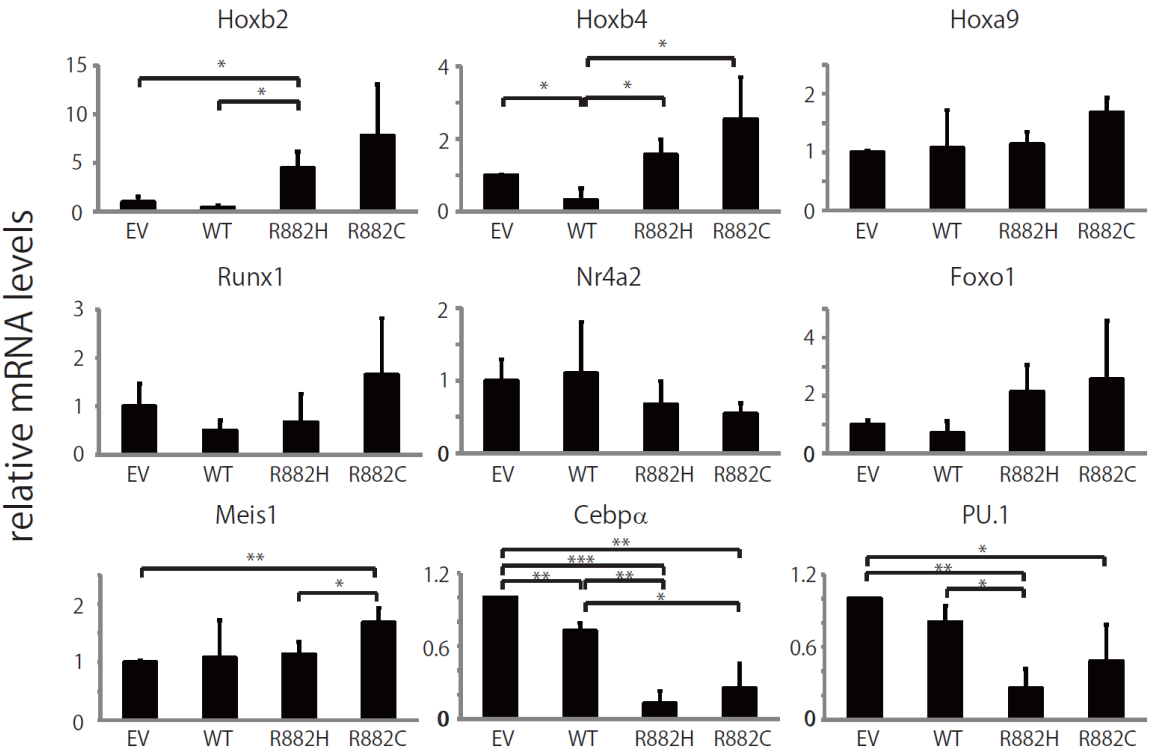

Figure 11. Relative expression levels of various hematopoiesis-associated genes in GFP+LSK cells measured by qPCR. (N = 3 replicate experiments, normalized to the expression levels in EV-transduced LSK cells.) Data are mean±SD values. *p<0.05, **p<0.01, ***p<0.001

Up-regulation of HSC self-renewal-associated genes and down-regulation of HSC differentiation-associated genes in DNMT3A R882 mutant-transduced stem/progenitor

cells highlight the phenotype of BMT experiments described above. Given that DNMT3A is a methyltransferase and R882 is located in the catalytic domain of DNMT3A, I subsequently analyzed DNA methylation status in vector-transduced stem/progenitor cells to elucidate whether the deregulated gene expression was due to altered DNA methylation status. Intracellular flow cytometry analysis revealed no significant difference in global 5-methylcytosine levels among four types of GFP+LK cells (Figure 12).

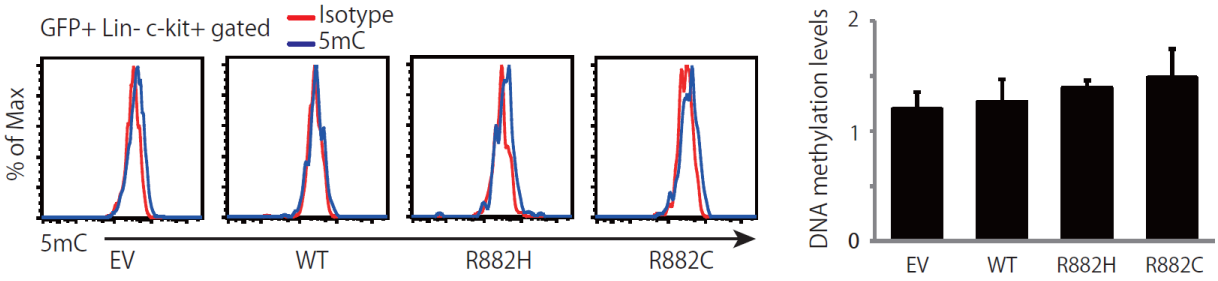

Figure 12. Representative flow cytometry histograms of total CpG methylation of GFP+LK cells using 5-methylcytosine-specific antibody (Left). Quantification of total CpG methylation status shown as normalized mean fluorescence intensity (Right). (N = 3 replicate experiments)

However, targeted bisulfite sequencing experiment using GFP+LSK cells showed hyper-methylation of the Hoxb2 promoter-associated CpG island in WT-transduced cells and hypo-methylation in R882H-transduced cells relative to EV-transduced control

cells (Figure 13). This altered CpG island methylation status was consistent with Hoxb2 mRNA expression of transplanted mice. On the other hand, the decreased mRNA expression of PU.1 in DNMT3A mutant-transduced LSK cells was not associated with CpG methylation status. DNMT3A R882H evoked no change in methylation status of PU.1 promoter-associated CpG island. (Figure 13).

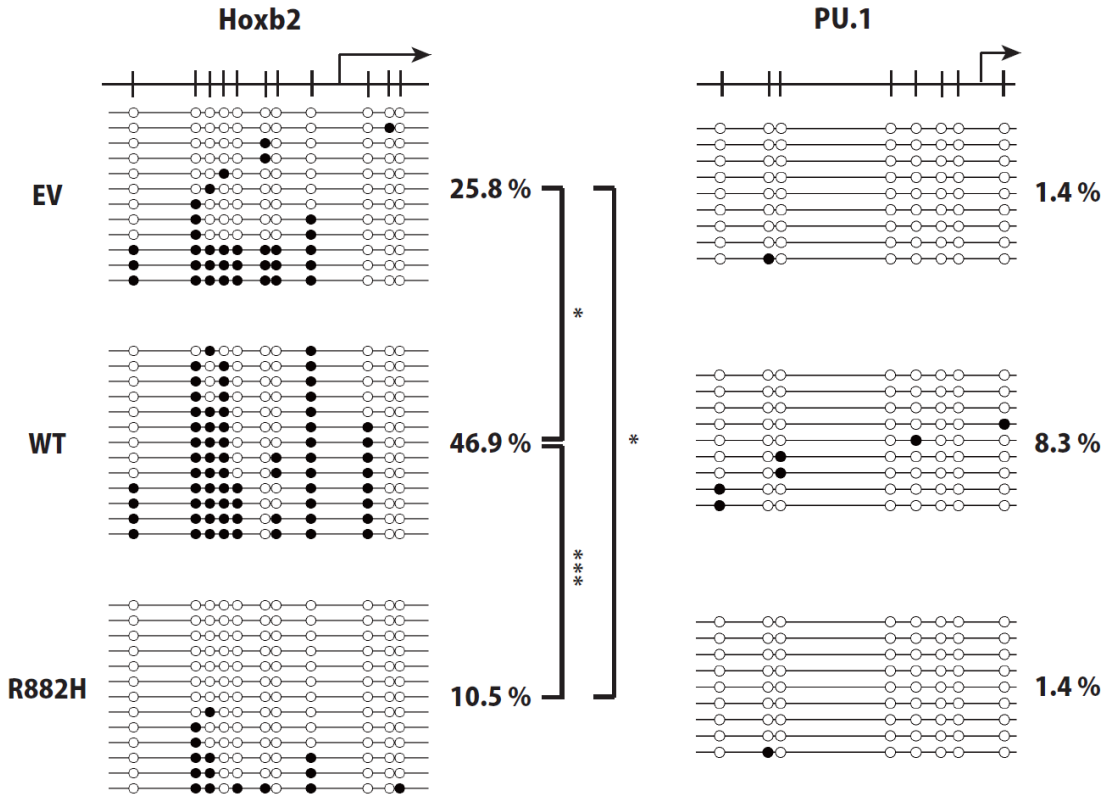

Figure 13. Bisulfite sequencing analysis of promoter-associated CpG island of Hoxb2 (Left) and PU.1 (Right) in GFP+LSK cells. Arrows represent transcription start sites. Open and filled circles represent unmethylated and methylated CpGs, respectively. Data are mean±SD values. *p<0.05, **p<0.01, ***p<0.001

These results from the selected genes' analysis indicate that DNMT3A R882 mutants have DNA methylation-independent mechanism that causes down-regulation of differentiation-associated genes in addition to DNA methylation-dependent effect that leads to CpG hypo-methylation, followed by up-regulation of HSC self-renewal-associated genes as shown in the previous Dnmt3a knockout mice study.

DNMT3A R882 mutation specifically interacts with Polycomb repressive complex 1.

As noted above, DNMT3A interacts with several histone modifiers to repress the target gene expression. Especially, previous reports showed that the recruitment of PRC1 complex is affected by DNMT1, a member of DNA methyltransferases[38], whereas most histone modifiers appear to be upstream landmarks of DNMT3A to catalyze DNA methylation[25,29]. Based on these facts, I hypothesized that the DNMT3A R882 mutants could alter the recruitment of collaborators to target gene loci, and I performed co-immunoprecipitation experiments using lysates from transiently transfected HEK 293T cells with expression vectors for DNMT3A WT or R882 mutants and several PRC1 components to elucidate the molecular mechanisms other than DNA

methylation. As with the analysis of transplanted mice, intracellular flow cytometry showed no difference in global 5-methylcytosine levels among four types of vector (EV, WT, R882H, R882C)-transfected HEK293T cells (Figure 14).

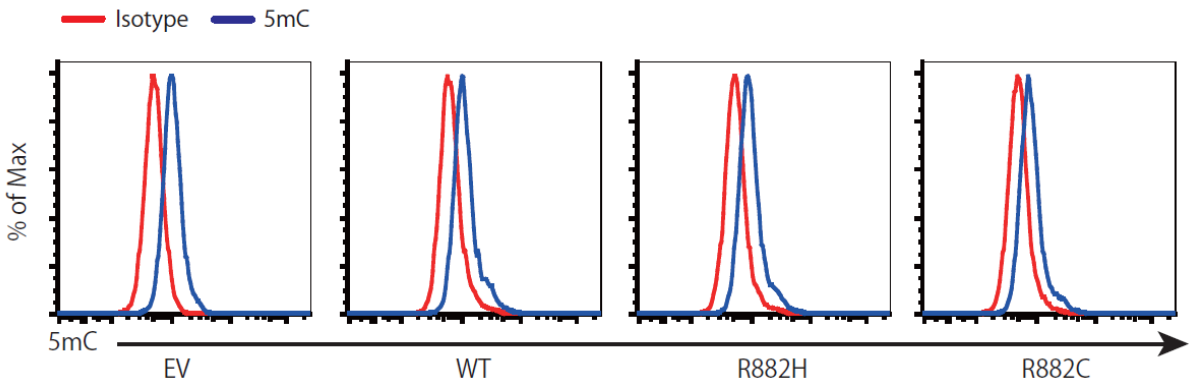

Figure 14. Representative flow cytometry histograms of total CpG methylation of HEK293T cells transfected with each vector using 5-methylcytosine-specific antibody.

Co-immunoprecipitation experiments showed that DNMT3A R882 mutant proteins had a greater affinity for BMI1 and RING1B, both of which are components of PRC1 complex, than DNMT3A WT protein (Figure 15A and 15B).

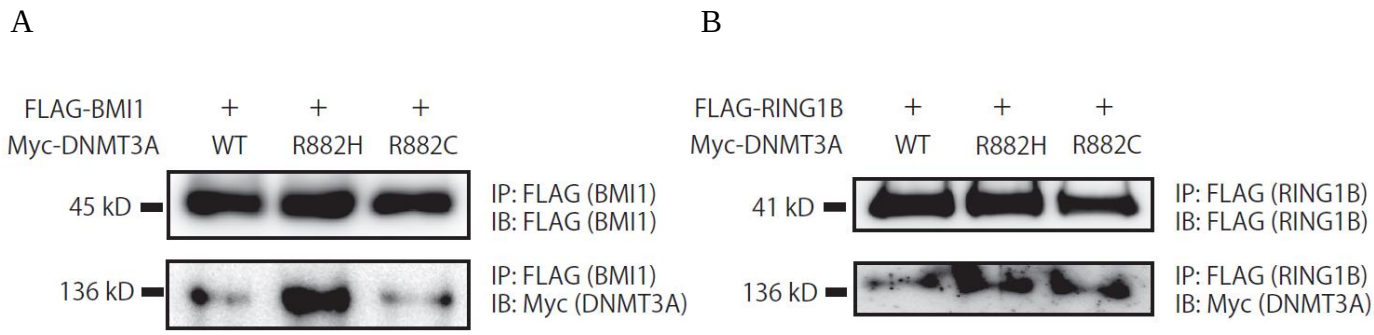

Figure 15. Extracts from HEK293T cells co-transfected with FLAG-BMI1 (A) or -RING1B (B), and Myc-DNMT3A WT or –R882 mutants are immunoprecipitated with anti-FLAG antibody and are immunoblotted with either anti-FLAG or anti-Myc antibody.

To further characterize the interaction between DNMT3A mutants and PRC1 complexes, I transiently transfected HEK293T cells with FLAG-tagged DNMT3A WT or R882 mutant alone and pulled down by antibody against several PRC1 components and anti-FLAG antibody. Interestingly, DNMT3A R882H and R882C mutant proteins exhibited augmented interaction with BMI1 and MEL18 (Figure 16A and 16B).

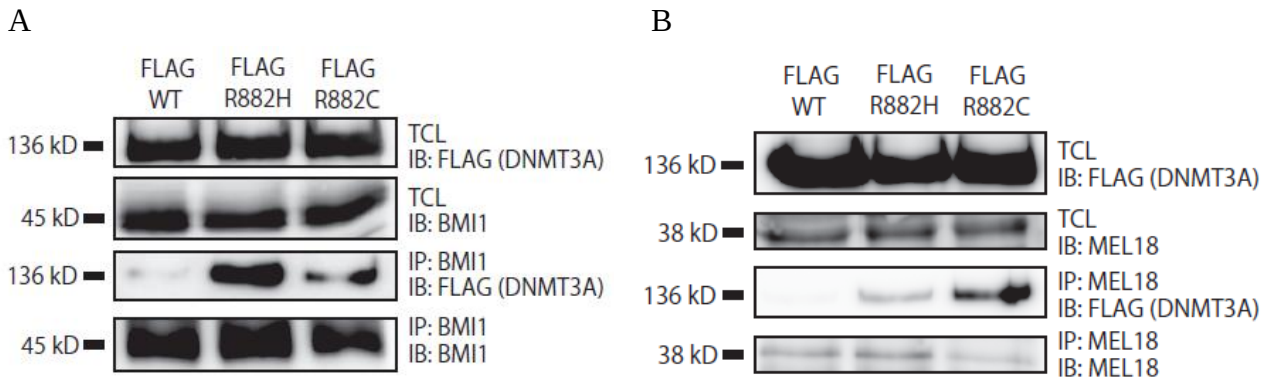

Figure 16. Extracts from HEK293T cells transfected with FLAG-DNMT3A WT or –R882 mutants are immunoprecipitated with anti-BMI1 (A) and MEL18 (B) antibody and are immunoblotted with anti-FLAG antibody.

BMI1 and MEL18 are structural homologues that belong to different PRC1 complexes, and both complexes maintain repression of gene expression by altering the chromatin status at specific promoters. Furthermore, RING1B, which is an essential common component of PRC1 complexes, was more firmly bound to DNMT3A R882 mutant than DNMT3A WT, irrespective of the type of amino acid substitution (Figure 17). These observations suggested that PRC1 complex favors DNMT3A R882 mutants over DNMT3A WT as a collaborating partner.

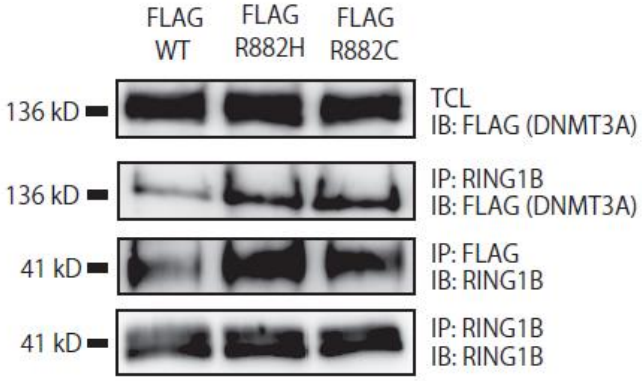

Figure 17. Extracts from HEK293T cells transfected with FLAG-DNMT3A WT or -R882 mutants are immunoprecipitated with anti-RING1B and FLAG antibody and are immunoblotted with anti-FLAG and RING1B antibody, respectively.

Previous reports have revealed that PRC1 complexes are divisible into two distinct types[39,40], one is PRC2-dependent PRC1 complex (PDPC) and another is PRC2-independent PRC1 complex (PIPC). CBX proteins recognize histone H3K27me3 and bind to these loci. Subsequently, PDPC represses the targeted gene expression through chromatin compaction and the placement of a repressive mark, histone H2AK119 ubiquitination. Therefore, to elucidate which PRC1 complex has enhanced interaction with DNMT3A R882 mutant, I pulled down the same sample with antibody against CBX7, a component of PDPC, and RYBP, a component of PIPC. Western blotting analysis revealed that DNMT3A R882 mutant (especially in R882H) had a greater affinity with CBX7 than DNMT3A WT (Figure 18A). On the other hand, no altered interaction between RYBP and DNMT3A R882 mutant was detected when

compared to DNMT3A WT (Figure 18B). These experiments characterized PDPC as a coordinating factor of DNMT3A R882 mutant.

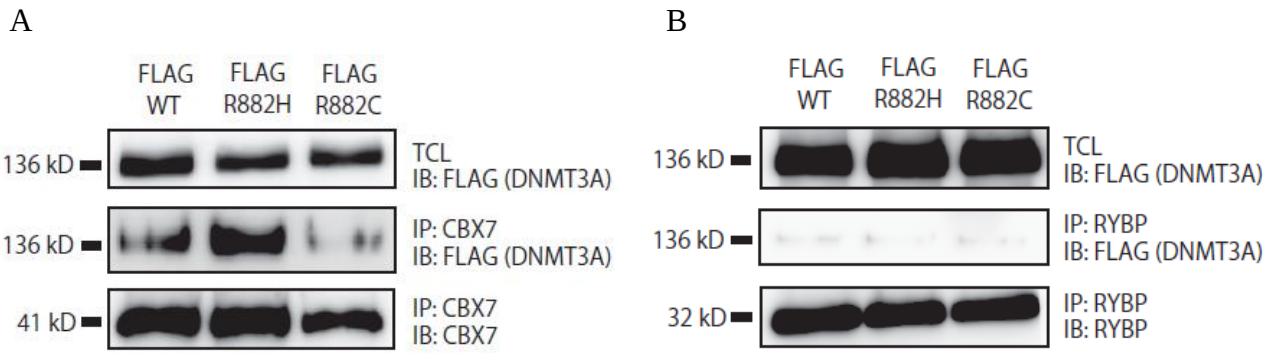

Figure 18. Extracts from HEK293T cells transfected with FLAG-DNMT3A WT or –R882 mutants are immunoprecipitated with anti-CBX7 (A) and RYBP (B) antibody and are immunoblotted with anti-FLAG antibody.

Finally, immunoprecipitation study revealed that an association between endogenous DNMT3A and MEL18 in OCI-AML3, a human AML cell line with DNMT3A R882C mutation (Figure 19) [41], which might emphasize the interaction between DNMT3A R882C and MEL18 in AML pathogenesis.

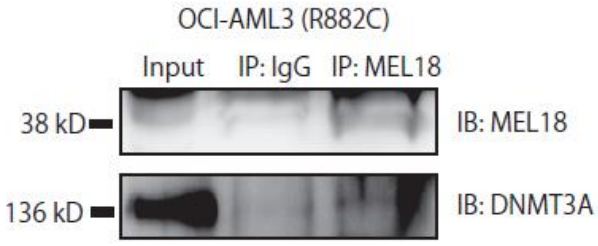

Figure 19. Endogenous interactions between DNMT3A R882C and MEL18. Extract from OCI-AML3 cells is immunoprecipitated with anti-MEL18 antibody or normal IgG and immunoblotted with anti-MEL18 or DNMT3A antibody.

Together, these results showed that DNMT3A R882 mutation had enhanced interaction with PDPC without altered global 5-methylcytosine levels.

PRC1 complex is required for DNMT3A mutation-induced stem cell accumulation through down-regulation of differentiation-associated genes.

To assess the importance of the PRC1 complex interaction in vivo in DNMT3A R882 mutant-induced aberrant HSC accumulation, I performed transplantation assay using Bmi1 hetero-KO ($Bmi1^{+/-}$) and Bmi1 WT ($Bmi1^{+/+}$) littermate control mice. Previous reports revealed that Bmi1-null HSCs lose their stem cell function critically, but heterozygosity has little effect on normal hematopoiesis[42,43]. I transplanted EV, WT,

or R882H-transduced c-kit+ mouse BM cells to lethally irradiated mice and analyzed these mice at four weeks post-transplant. Strikingly, heterozygosity of Bmi1 canceled the effect of DNMT3A R882 mutation without influence on EV-transduced HSC (Figure 20A and 20B), indicating that normal expression level of Bmi1 is required for DNMT3A R882 mutant-induced HSC accumulation.

A

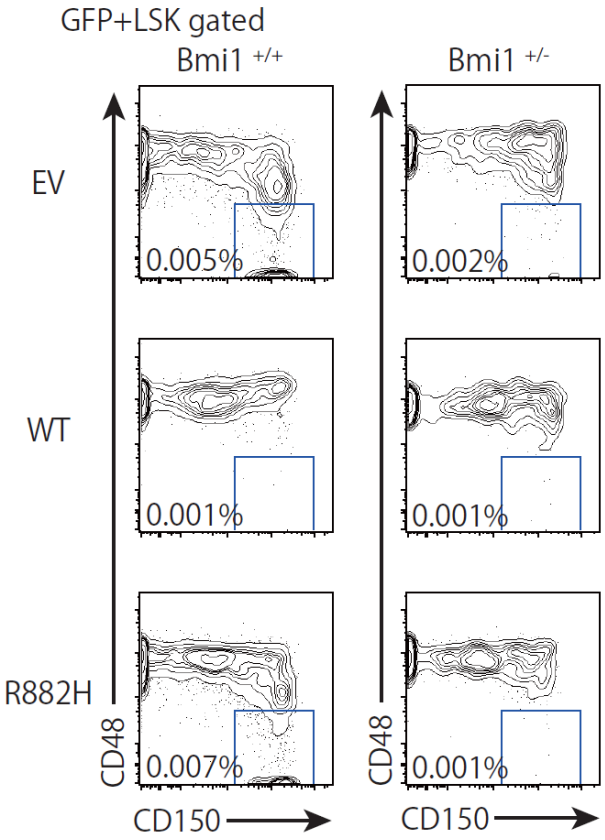

B

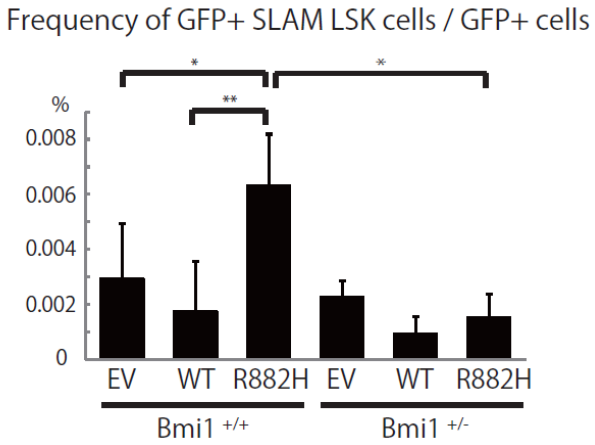

Figure 20. (A) Representative flow cytometry data of BM cells obtained from mouse transplanted with Bmi1$^{+/+}$ (Left) or Bmi1$^{+/-}$ (Right) cells transduced with EV, DNMT3A WT, or DNMT3A R882H. The boxed region shows the frequency of GFP+SLAM LSK cells in GFP+ cells. (B) Cumulative data of the frequency of GFP+SLAM LSK cells in GFP+ cells. (N = 4 mice). Data are mean±SD values. *p<0.05, **p<0.01

I also sorted GFP+LSK cells from these mice and performed qPCR to assess the expression of potent target genes described above. Hoxb cluster genes, especially Hoxb2, were up-regulated in R882H-transduced LSK cells, irrespective of Bmi1 genotype. Interestingly, Bmi1 heterozygosity restored the expression levels of down-regulated myeloid differentiation-associated genes (especially in PU.1) to normal levels in R882 mutant-transduced cells (Figure 21).

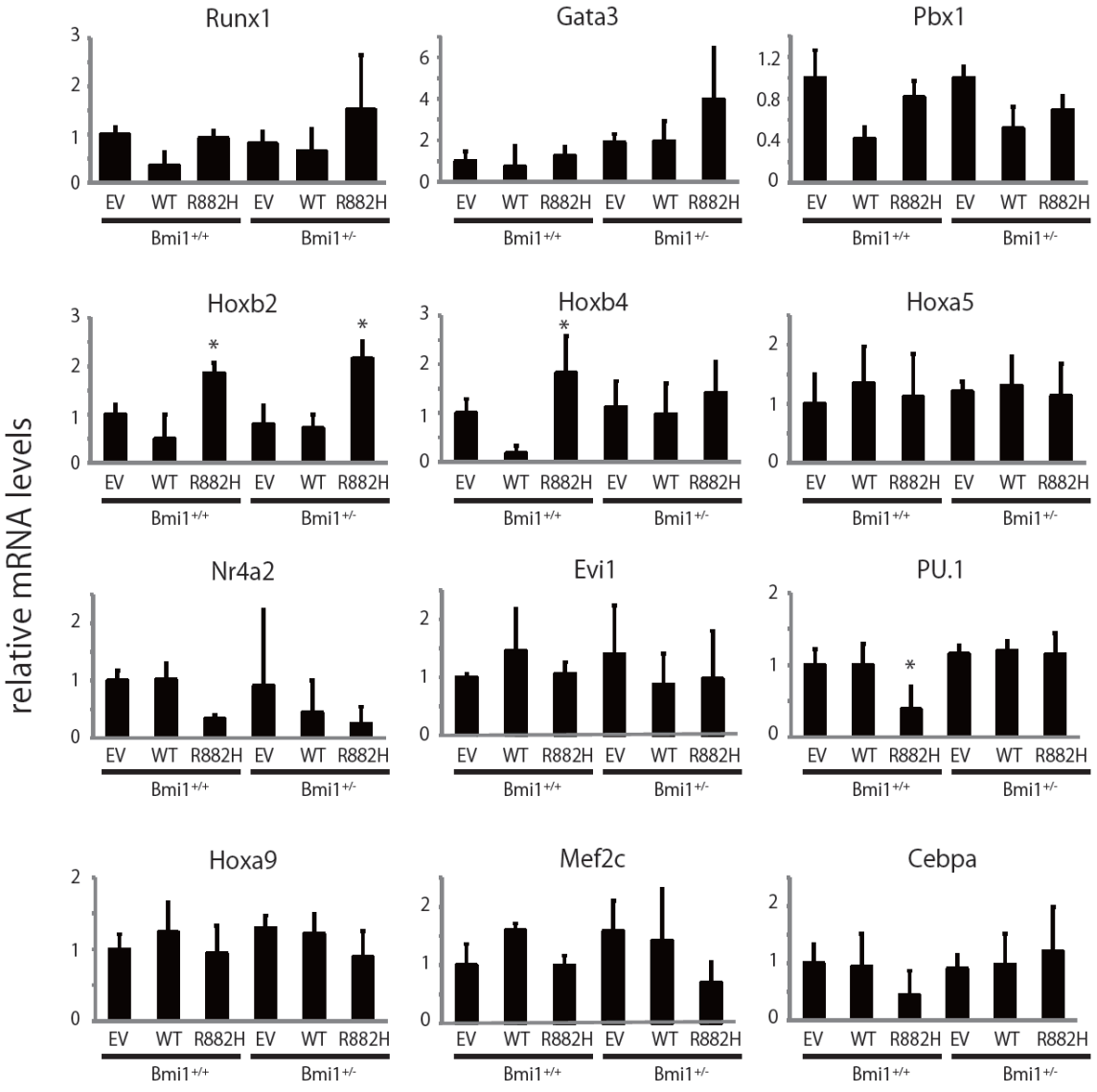

Figure 21. Relative expression levels of various hematopoiesis-associated genes in GFP+KSL cells measured by qPCR. (N = 3 replicate experiments, normalized to the expression levels in EV-transduced LSK cells.) Data are mean±SD values. *p<0.05

These findings suggested that the augmented interaction between DNMT3A R882 mutant and PRC1 complex was responsible for R882 mutant-induced HSC accumulation in vivo through silencing of differentiation-associated genes. Therefore, I

performed secondary BMT assay using murine PU.1 expression vector. KuOr-labeled EV, WT, or R882H-transduced c-kit+ cells sorted from primary recipient mice were transduced with EV or PU.1 (detected by GFP fluorescent protein). Subsequently, I transplanted double-transduced (GFP+KuOr+) cells to lethally irradiated mice (Figure 22).

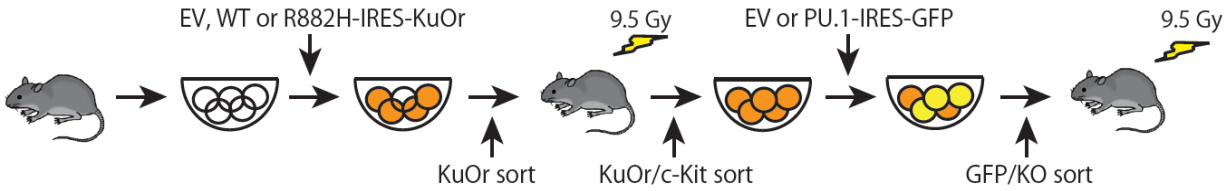

Figure 22. Design of competitive repopulating assay in secondary recipient mice transplanted with EV- or PU.1-transduced EV-, DNMT3A WT-, or DNMT3A R882H-transduced c-kit+ cells obtained from primary recipient mice.

The assessment of PB chimerism at four weeks post-transplant in each recipient group revealed that DNMT3A R882H-transduced stem/progenitor cells had a slightly but significantly higher repopulating capacity compared to EV control, and exogenous PU.1 expression almost totally impaired the repopulating capacity of EV and R882H-transduced cells, suggesting the functional role of PU.1 in the altered hematopoiesis by DNMT3A R882H (Figure 23).

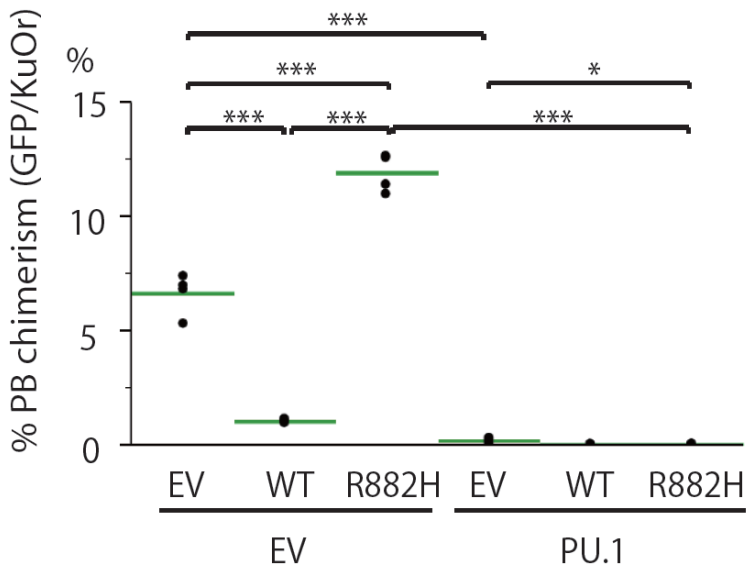

Figure 23. Contribution of EV, and PU.1 to PB chimerism at four weeks after transplantation in secondary recipients. (N = 4 mice). Data are mean±SD values. *p<0.05, **p<0.01, ***p<0.001

To confirm that PU.1 is a direct target of aberrant collaboration between DNMT3A R882 mutant and PRC1 complex, I performed chromatin immunoprecipitation (ChIP)-qPCR experiment using HL-60 cells transduced with doxycycline-inducible DNMT3A WT or R882H mutant (Figure 24).

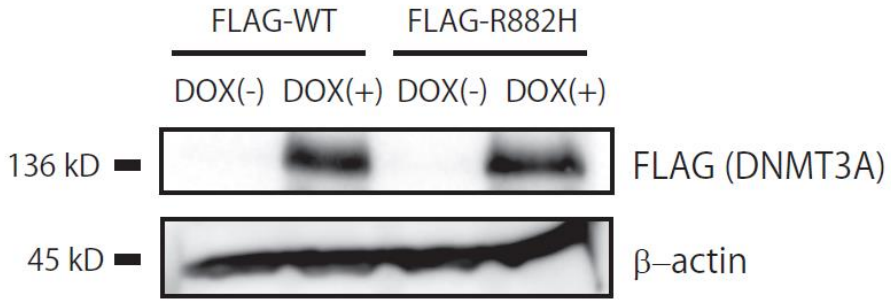

Figure 24. Protein expression of HL-60 cells transduced with doxycycline-inducible FLAG-tagged DNMT3A WT or R882H with or without administration of doxycycline using anti-FLAG antibody. β-actin was blotted as a loading control.

Because it took only five days for myeloid differentiation of HL-60 cells by the transduction of DNMT3A WT (Figure 3), I utilized doxycycline-inducible vector and analyzed the undifferentiated HL-60 cells at day 3 post doxycycline induction. ChIP-qPCR experiment using crosslinked cells three days after doxycycline administration revealed that BMI1 and RING1B were more efficiently recruited to the upstream regulatory element (URE) of PU.1 upon expression of DNMT3A R882H than DNMT3A WT, while the amount of DNMT3A recruited were comparable between DNMT3A WT and R882H. In addition, RING1B-mediated ubiquitination of histone H2AK119 was more enriched at the same locus in DNMT3A R882H mutant-transduced HL-60 cells (Figure 25).

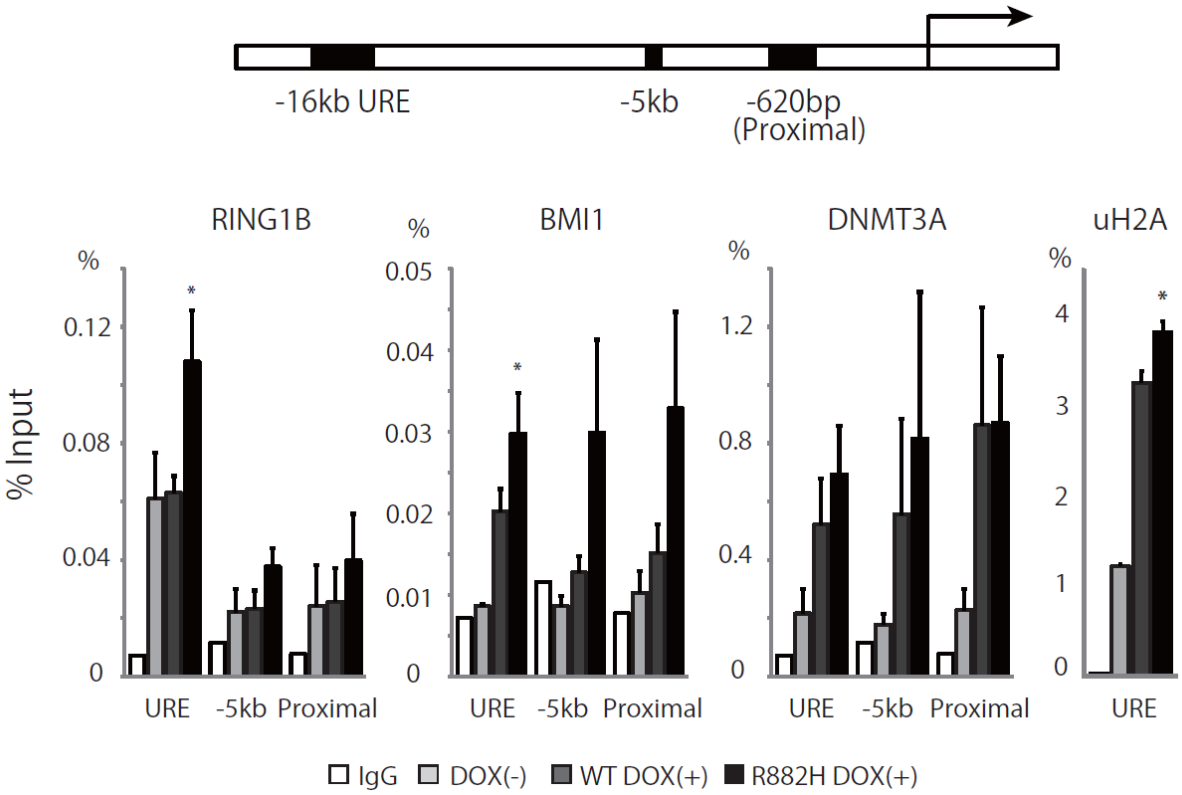

Figure 25. ChIP-qPCR experiment of the PRC1 components BMI1 and RING1B, DNMT3A, and ubiquitinated H2A in HL-60 cells at the URE, a 5kb upstream region, and proximal promoter region of PU.1 in the absence of or in the presence of either doxycycline-inducible DNMT3A WT or DNMT3A R882H. (N = 3 replicate experiments except for IgG control (N=1) and ubiquitinated H2A in DOX(-) (N=2)) Data are mean±SD values. *p<0.05 between WT DOX(+) and R882H DOX(+).

From these results, it is supposed that transcriptional silencing of PU.1 comes from increased URE occupancy of PRC1 complex upon expression of DNMT3A R882H. Furthermore, these data suggest that enhanced interaction between DNMT3A R882 mutant and PRC1 complex decreases mRNA levels of myeloid differentiation-associated genes, which might play a positive role in the increased frequency of DNMT3A R882 mutant-transduced HSCs.

PRC1 complex is essential to development, maintenance, and ATRA resistance of DNMT3A mutant-associated leukemic cells.

As revealed above, DNMT3A R882 mutant alone is insufficient to cause leukemic transformation in vitro and in vivo (Figure 6 and Figure 8). Therefore, I searched some potent collaborating genes for development of AML from public database, resulting the finding that HOXA and HOXB cluster genes were highly expressed in clinical AML samples harboring DNMT3A mutation[8,44]. From my mice study, Hoxb cluster genes were up-regulated in DNMT3A R882 mutant-transduced murine HSCs, but Hoxa cluster genes were not altered by DNMT3A mutant alone (Figure 11). As exogenous expression of HOXA9 induces immortalization in methylcellulose assay and myeloproliferative disease in vivo[45], I co-transduced DNMT3A and HOXA9 to mouse BM c-kit+ cells and performed colony replating assay to assess whether DNMT3A mutation had an additional effect on HOXA9-induced myeloproliferative disease (Figure 26).

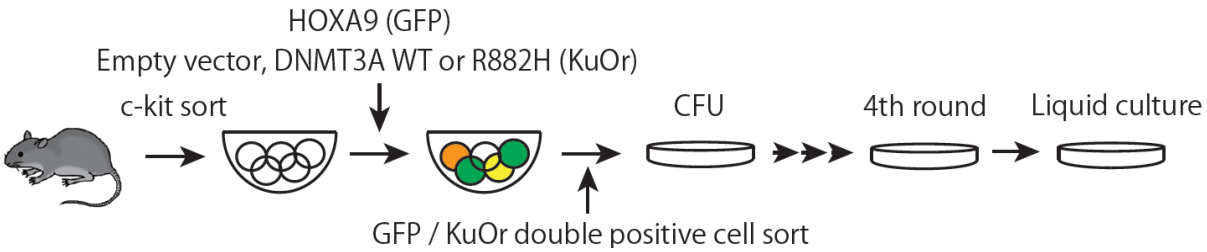

Figure 26. Design of CFU and liquid culture assay with HOXA9 and EV-, DNMT3A WT-, or DNMT3A R882 mutant-transduced c-kit sorted murine BM cells.

In in vitro colony replating assay, DNMT3A WT and HOXA9 co-transduced cells had no colony formation at third replating whereas BM cells transduced with HOXA9 plus EV or DNMT3A R882H could easily be replated multiple times (immortalized) and generated large colonies than DNMT3A WT and HOXA9 co-transduced cells (data not shown). After the fourth round of replating, immortalized cells were transferred to liquid culture containing IL-3. While HOXA9 and EV co-transduced cells showed a decline in cell growth from three days after the transfer, HOXA9 plus R882H transduced immortalized cells slowly but steadily proliferated for one week, indicating the proliferative advantage of DNMT3A R882H in concert with HOXA9 (Figure 27).

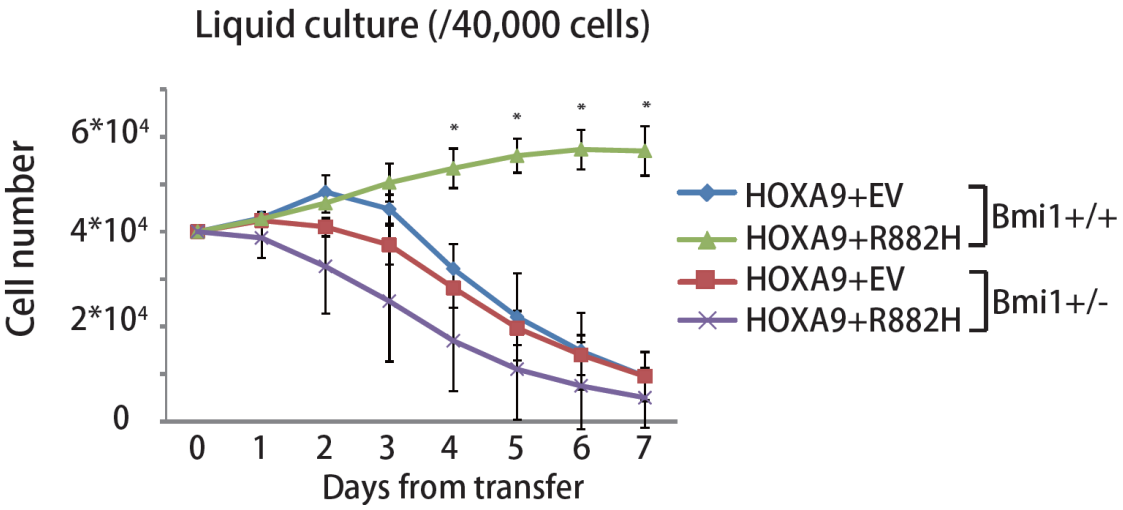

Figure 27. Growth curve of Bmi1$^{+/+}$ and Bmi1$^{+/-}$ murine immortalized cells transduced with HOXA9 and EV or DNMT3A R882H in liquid culture. (N = 3 replicate experiments) Data are mean±SD values. *p<0.05

Morphological and surface marker analysis of these immortalized cells revealed that the most of HOXA9 and EV co-transduced cells were mature granulocytes, monocytes and macrophages and that HOXA9 and DNMT3A R882H co-transduced cells were mainly F4/80+, Mac1+, Gr1- monocytic blasts, consistent with clinical observation that DNMT3A mutation is found frequently in FAB M4/M5 leukemia (Figure 28A and 28B).

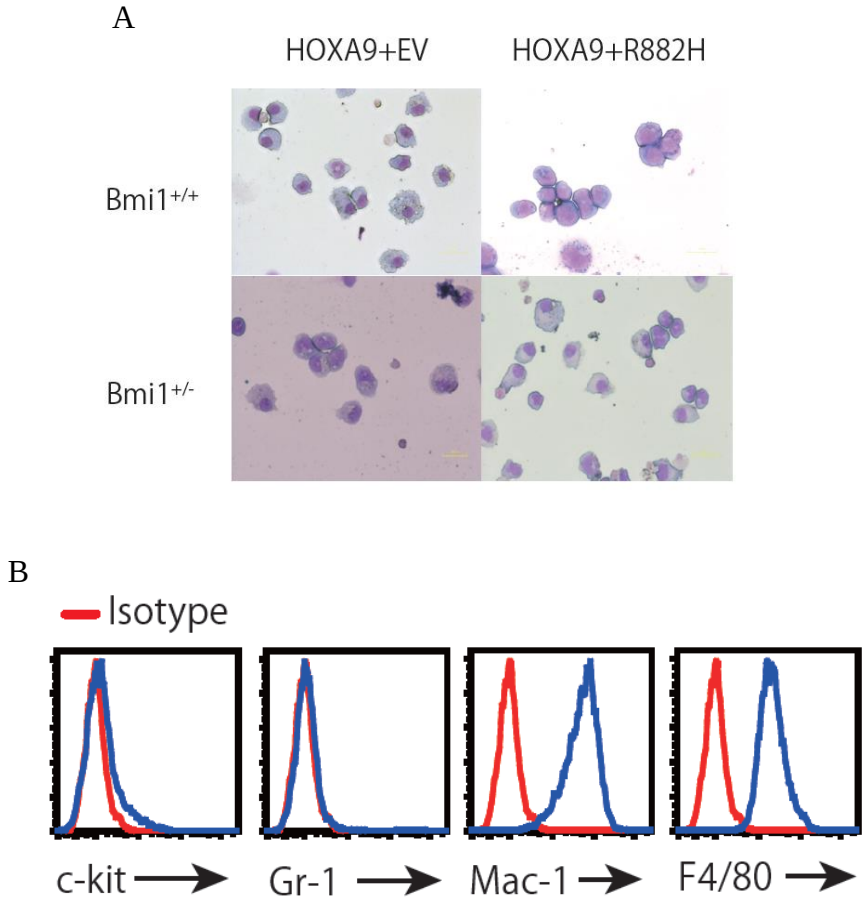

Figure 28. (A) Typical morphology of Bmi1$^{+/+}$ and Bmi1$^{+/-}$ murine immortalized cells transduced with HOXA9 and EV or DNMT3A R882H in liquid culture. (B) Representative surface maker of Bmi1$^{+/+}$ murine immortalized cells transduced with HOXA9 and DNMT3A R882H.

These results indicate a distinct role for DNMT3A mutation as well as a potential collaboration between DNMT3A R882H and HOXA9 in malignant transformation of hematopoietic cells. Subsequently, I assessed the impact of PRC1 complex on this monoblastic transformation using Bmi1$^{+/-}$ and Bmi1$^{+/+}$ littermate control mice. Although BM cells transduced with HOXA9 plus EV or DNMT3A R882H

immortalized, irrespective of Bmi1 genotype, Bmi1 heterozygosity reduced the colony number of HOXA9 and R882H co-transduced cells at the first round (Figure 29).

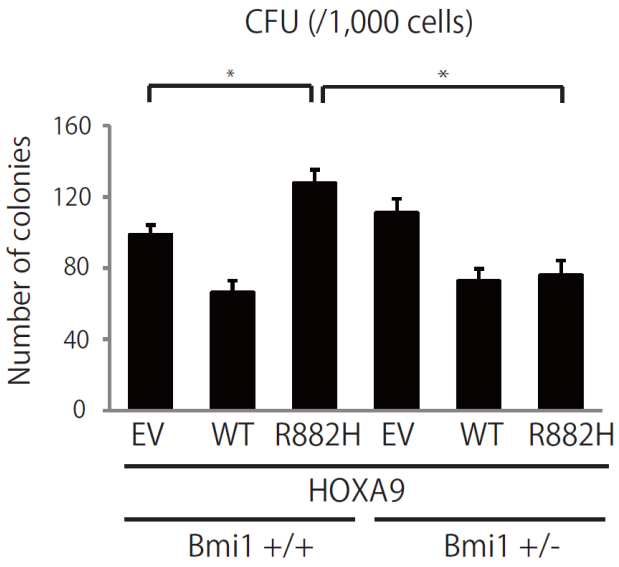

Figure 29. Cumulative colony-forming capacity is shown for an initial plating of 1000 co-transgene-expressing cells. (N = 3 replicate plates). Data are mean±SD values. *p<0.05

Furthermore, Bmi1 heterozygosity impaired monoblastic transforming capacity and growth advantage of HOXA9 and R882H co-transduced progenitors. Wright-Giemsa staining showed that cells from HOXA9 and R882H co-transduced Bmi-$1^{+/-}$ -derived third round colonies were fully composed of mature macrophages and granulocytes (Figure 27 and 28A). These results suggested that normal expression level

of Bmi1 is also indispensable for the differentiation block of DNMT3A R882H and HOXA9 co-transduced murine BM cells.

In order to investigate the importance of PRC1 complex for maintenance and ATRA-resistance of DNMT3A-mutated AML, I next designed two shRNAs targeting RING1B, and retrovirally transduced these vectors to OCI-AML3 (DNMT3A mutated) and THP1 (DNMT3A not mutated) cell lines, and HL-60 cells were transduced with doxycycline-inducible DNMT3A WT or R882H. Western blotting analysis of RING1B in HL-60 cells showed a 50-60% reduction of RING1B compared to the control shRNA vector-transduced HL-60 cells (Figure 30).

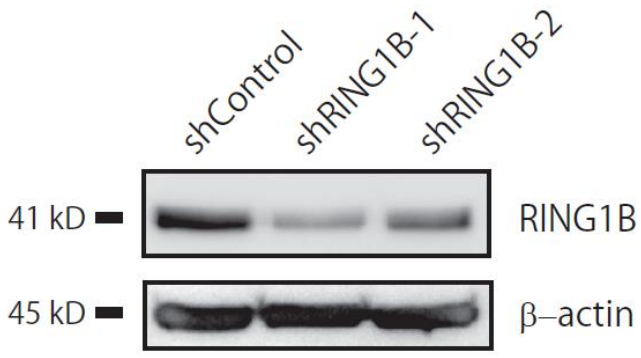

Figure 30. Protein expression of HL-60 cells transduced with shControl, shRING1B-1, or shRING1B-2 using anti-RING1B antibody. β-actin was blotted as a loading control.

RING1B knockdown significantly showed a decreased proliferative capacity of OCI-AML3 cells (Figure 31A). Wright-Giemsa staining of these cells revealed that OCI-AML3 cells expressing RING1B shRNA were mature cells morphologically as typified by small cell size, reduced nucleus-to-cytoplasm ratio, and segmented nucleus (Figure 32). When the same setting of RING1B knockdown was applied to THP1 cells, a monocytic AML cell line not carrying DNMT3A mutation[46], reduction in RING1B expression did not affect the proliferation rate and morphology in THP1 cells (Figure 31B). These experiments suggested that RING1B plays an essential role for maintenance of DNMT3A-mutated monocytic AML cell line.

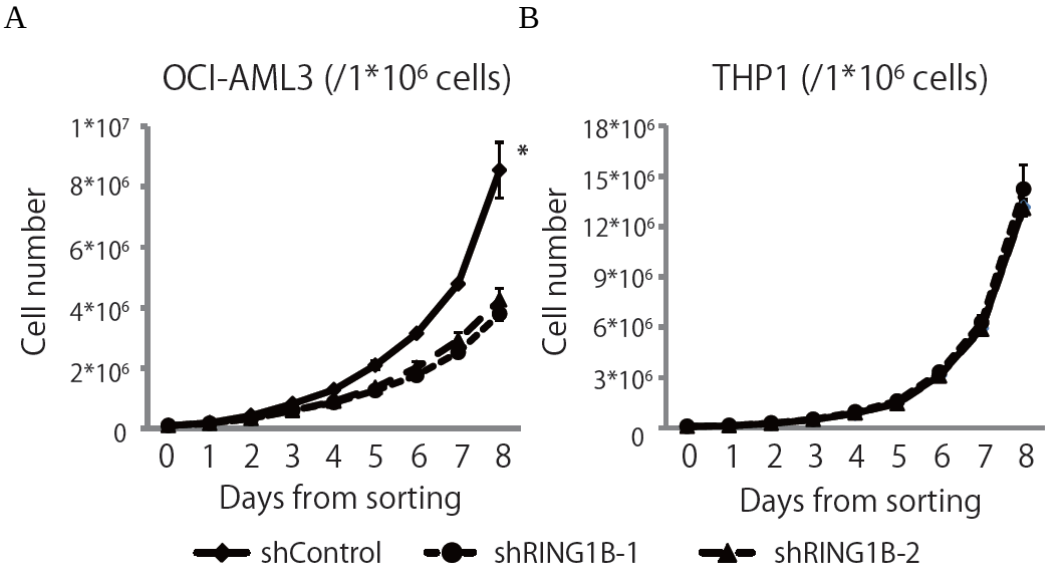

Figure 31. Growth curve of OCI-AML3 (A) and THP1 cells (B) transduced with shControl or shRING1B. (N = 3 replicate experiments) Data are mean±SD values. *p<0.05

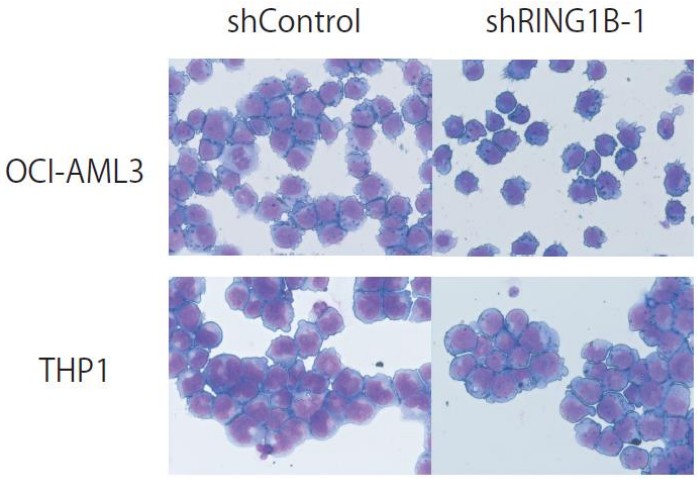

Figure 32. Typical morphology of OCI-AML3 and THP1 cells transduced with shControl or shRING1B-1.

In experiments using HL-60 cells transduced with doxycycline-inducible DNMT3A WT or R882H, knockdown of RING1B eliminated the distinction between WT- and R882H-transduced cells in the growth curve and the difference between R882H-non expressed and R882H-expressed cells in the sensitivity to ATRA, although it was possible that RING1B could have its own effectors on the proliferative capacity and the expression of CD11b of HL-60 in DNMT3A mutant-independent manner (Figure 33A, 33B, and 33C).

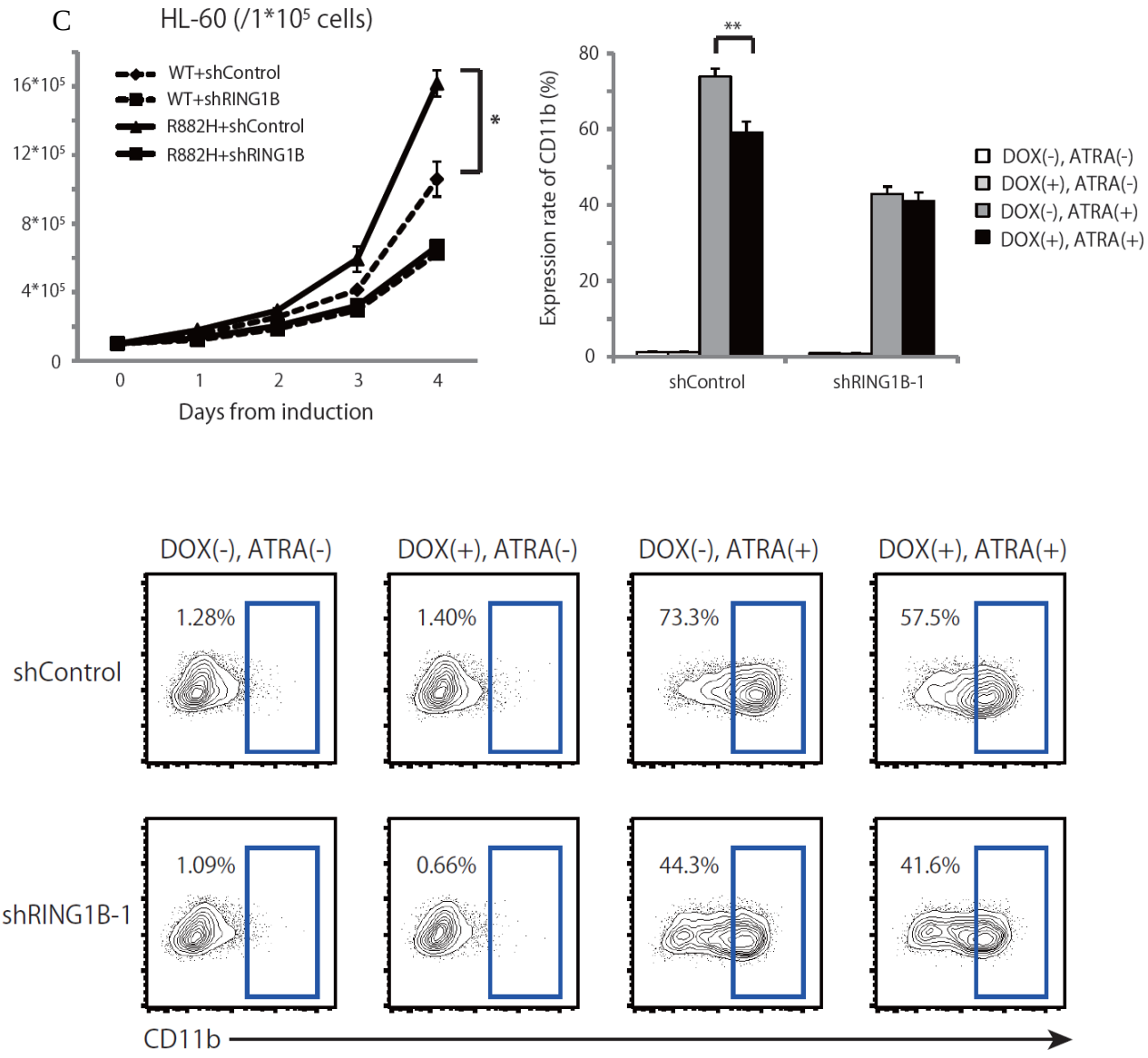

Figure 33. (A) Growth curve of HL-60 cells transduced with doxycycline-inducible DNMT3A WT or DNMT3A R882H, and shControl or shRING1B. (N = 3 replicate experiments) (B) Cumulative data of CD11b positivity rate 48 h after doxycycline-induced transgene expression and administration of ATRA (1μM) or EtOH. (N = 3 replicate experiments) (C) Representative surface maker CD11b expression of HL-60 cells transduced with doxycycline-inducible DNMT3A WT or R882H, and shControl or shRING1B at 48 h after doxycycline-induced transgene expression and administration of ATRA (1μM) or EtOH. Data are mean±SD values. *p<0.05, **p<0.01

In summary, these results demonstrate that PRC1 complex is necessary for monoblastic transformation of BM progenitors with DNMT3A R882 mutant and HOXA9 overexpression, for differentiation block, and for resistance to differentiation-inducing therapy of DNMT3A-mutated AML cells.

Discussion

The data presented here identified that DNMT3A R882 mutation results in differentiation block of HSCs and leukemic cells, and promoting leukemic transformation in combination with HOXA9 via aberrant recruitment of PRC1 complex to specific differentiation-associated gene loci.

DNMT3A mutation has been so far thought to be a loss-of-function mutation due to the reduced DNA methyltransferase activity of purified DNMT3A R882 mutant protein and the premature truncated protein translated from the remaining mutations[8]. Several evidence regarding DNMT3A mutant in AML as described below have prompted me to hypothesize that DNMT3A R882 mutation has certain gain-of-function and/or dominant-negative effects: (1) The most prevalence of R882 mutation up to 60% in DNMT3A-mutated AML; (2) Heterozygous DNMT3A R882 mutations as the most frequent genotype in AML; (3) No apparent phenotype in Dnmt3a hetero-knockout mice[47]. To test my hypothesis, I utilized viral overexpression system for the forced expression of DNMT3A mutations into primary murine cells and cell lines. In the system, DNMT3A mutants were successfully and functionally analyzed by comparing samples with forced expression of empty vector or DNMT3A WT, although there lied

some limitations regarding the system such as the relatively higher level of DNMT3A expression than human primary AML samples and the vector-derived insertional mutagenesis. In fact, I found that DNMT3A R882 mutant contributed to insensitivity to ATRA-induced differentiation of AML cell lines and promoted monoblastic transformation of normal stem/progenitor cells in combination with HOXA9, while EV and HOXA9 co-transduced cells did not transform. From my murine BMT assays, aberrant expression of DNMT3A R882 mutant alone was insufficient for leukemia development indicating that DNMT3A R882 mutant would require one or more additional genetic events to develop myeloid malignancies. Indeed, some recent studies revealed that DNMT3A mutations are identified as an early genetic event and remarkably stable during AML evolution[48-50]. Furthermore, somatic mutations of DNMT3A are shown to be detected in blood cells from healthy elderly individual and the donor cells of HSC transplantation[51,52], consistent with our findings that accumulated HSCs evoked by DNMT3A R882 mutant are in a quiescent state. With the fact that DNMT3A-mutated hematological diseases comprise not only AML but also myelodysplastic syndrome, and T-cell leukemia/lymphoma, it is also suspected that the altered genetic and epigenetic mechanism in HSC by DNMT3A mutation would form the backbone of premalignant status of HSCs. As described above, patients harboring

DNMT3A mutations frequently have NPM1 mutations. The previous report showed that NPM1 mutant knock-in allele in mouse hematopoietic cells causes up-regulation of Hoxa9 in mice[53]. Because HOXA9 is overexpressed in DNMT3A-mutated AML samples, but not altered in DNMT3A mutant-transduced murine LSK cells, I selected HOXA9 as a potential collaborating oncogene. As a result, I found that DNMT3A R882 mutant blocks myeloid differentiation and promote monoblastic transformation when combined with HOXA9.

Based on my findings, I propose that DNMT3A R882 mutant has two distinct mechanisms for leukemogenesis: (1) DNA methylation-dependent effect, leading to DNA hypo-methylation; (2) DNA methylation-independent effect, recruiting the PRC1 complex to specific target loci. Firstly, as an indicator of DNA methylation-dependent effect, exogenous expression of DNMT3A R882 mutant caused up-regulation of Hoxb2 with accompanying hypo-methylation of the promoter-associated CpG island in murine stem/progenitor cells possibly due to the disruption of DNMT3A tetramerization capacity[13], consistent with previous analysis using patient samples[8]. Secondary, as an indicator of DNA methylation-independent mechanism, my data indicated that DNMT3A R882 mutation-mediated recruitment of PRC1 complex to specific target loci

suppressed the expression of differentiation-associated genes, blocking differentiation of HSCs and leukemic cells (Figure 34).

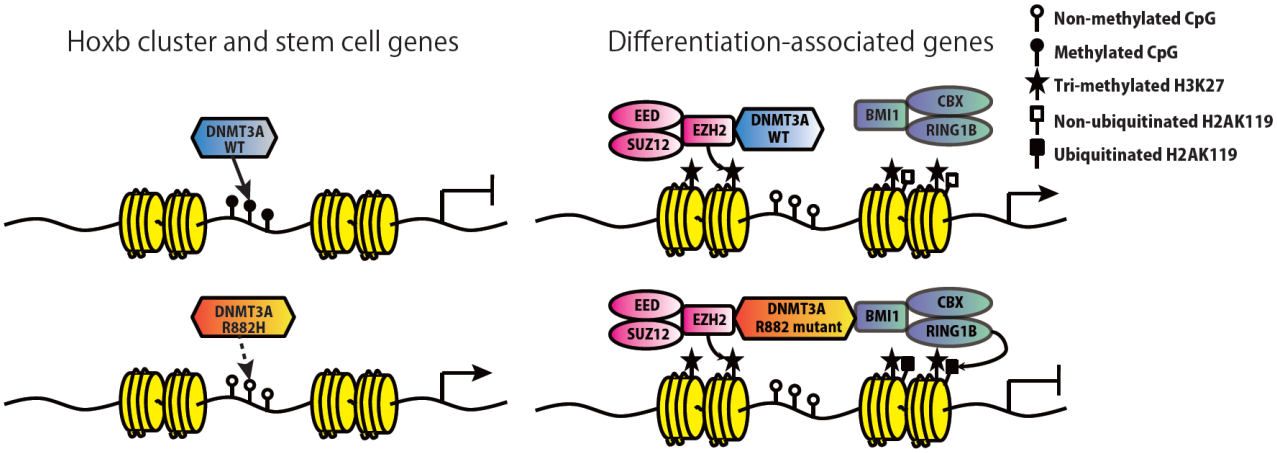

Figure 34. Schematic model of aberrant collaboration between DNMT3A R882 mutant and PRC1 complex in promoting differentiation block in HSCs and leukemic cells. Hoxb cluster genes, stem cell genes, and differentiation-associated genes are direct targets of DNMT3A. When HSCs or leukemic cells receive a differentiation signal, DNMT3A WT methylates these genes' promoter-associated CpG island and suppresses their mRNA transcription, leading to hematopoietic differentiation to progenitors and mature blood cells (Upper left). DNMT3A R882 mutant not only is incapable of methylating these regions but also disrupt the normal function of remaining WT allele, leading to up-regulation of these target genes, especially Hoxb2 (Left lower). Furthermore, DNMT3A R882 mutant recruits PDPC to the regulatory region of differentiation-associated genes. PDPC recruited by DNMT3A R882 mutant silence these genes' expression through the placement of a repressive mark, ubiquitinated H2AK119 contributing to the development of pre-leukemic state (HSC accumulation), leukemic state (monoblastic transformation), and therapy resistance (insensitivity to ATRA) (Right).

Based on the fact that Hoxb4 is a well-known inducer of HSC self-renewal in mice[54], it is possible that transcriptional activation of Hoxb cluster mediated by DNMT3A mutant causes expansion of stem cell fraction. However, considering the quiescent status of DNMT3A mutant-transduced HSCs with no proliferative advantage in colony formation, I additionally hypothesized that down-regulation of differentiation-associated genes was more important for the phenotypes described above. Indeed, I identified that DNMT3A R882 mutant-induced insensitivity to ATRA in HL-60 cells, aberrant HSC accumulation, and monoblastic transformation were abrogated by suppression of PRC1 complex as represented by Bmi1 heterozygosity and knockdown of RING1B.

Many studies utilizing knockout mouse of several components of PRC1 subunit revealed that PRC1 complex plays a crucial role for HSC self-renewal and differentiation through ubiquitination of histone H2AK119 and chromatin compaction in the last decade[55,56]. Especially, Bmi1 is well known to be an important regulator of HSC and some kind of leukemia stem cell self-renewal. Bmi1-null HSCs lose their long-term repopulating capacity and cause postnatal pancytopenia and death within 2 months after birth, while its heterozygosity has less impact on normal hematopoiesis[42,43]. On the other hand, Bmi1 deficiency reduces a clonogenic and proliferative capacity of

AML1-ETO, PLZF-RARα, and MLL-AF9 oncogenes causing immortalization of normal progenitors in vitro[57,58]. In addition, the previous study reported that heterozygosity of Bmi1 reduces Eμ-myc transgene-induced lymphomagenesis in mice[59]. Similarly, I found that Bmi1 heterozygosity counteracted the accumulation of HSC frequency by DNMT3A R882 mutant but that Bmi1 heterozygosity had no apparent impact on HSC frequency in mice transplanted with EV-transduced cells. Overexpression of BMI1 is commonly found in several hematological malignancies and correlates with disease prognosis[60], however, recurrent somatic mutations in PRC1 components have not been reported[61]. Given these clinical evidences, endogenous or higher expression of PRC1 complex would be essential for development and maintenance of not only DNMT3A R882-mutated AML but also a wide range of hematological diseases.

As described above, several recent reports have revealed that PRC1 complexes are classified into two distinct groups, PDPC and PIPC. The genome-wide localization of Cbx7 (representative for PDPC) and Rybp (representative for PIPC) showed that both complexes co-localize at many of the same loci, but also target the independent genes in mouse ESCs[62]. My immunoprecipitation analysis indicated that only PDPC was associated with DNMT3A R882 mutant-induced several phenotypes. In ESCs, PIPC

targets are enriched in germline regulator genes, whereas PDPC target are enriched in cell differentiation-, lineage commitment-, and developmental regulator-associated genes in line with my observation[62], although further study concerning the functional role of each complexes including genome-wide occupancy analysis in hematopoietic cells is remained to be done. In fact, I found that DNMT3A R882 mutant-associated PRC1 complex had a higher affinity to the PU.1 URE region, indicating that PDPC-based transcription silencing mechanism in cell differentiation and lineage commitment could be applied to the hematopoietic system. PU.1 is one of the most essential transcription factors of hematopoietic lineage development, and is required for the maturation of common myeloid progenitor and granulocyte-monocyte progenitor[63]. Inactivating mutation of PU.1 is detected in 7% of AML patients, and enriched in FAB M4/M5 AML as with the case of DNMT3A mutation[64]. In addition, down-regulation of PU.1 is also associated with leukemogenesis of several important oncogenes, such as AML1-ETO, FLT3-ITD, MN1, and PML-RARα[65-68]. Especially, exogenous expression of MN1 suppresses PU.1 expression and inhibits its activation by ATRA, promoting resistance to ATRA-induced differentiation in hematopoietic cells, consistent with my findings[67]. Based on the result that MN1 expression levels predict ATRA-resistance in patients with AML[67], it is important to verify the insensitivity to

differentiation-inducing therapy in DNMT3A-mutated AML cells using patient samples.

In summary, my study has revealed that the mechanism of DNMT3A mutant to promote leukemogenesis via collaborating with PRC1 complex for transcriptional silencing of differentiation-associated genes. This accomplishment of the functional analysis of DNMT3A mutant by overexpression system could tie in the concept generating heterozygous DNMT3A R882 mutant knock-in mouse model to cover the precise biological and molecular mechanism of DNMT3A mutant and PRC1 complex. The knock-in mouse model would be expected to overcome some limitations of this study in that the model could validate whether the endogenous expression of mutated DNMT3A protein possesses the similar function to overexpressed DNMT3A mutant. It is also to be addressed in the future how PRC1 complex is recruited to DNMT3A mutant target genes. Even considered that BMI1 is essential for normal hematopoiesis, attenuating the functional cooperation between DNMT3A mutant and PRC1 complex could be a promising therapeutic target in DNMT3A-mutated hematological malignancies.

Acknowledgements

I express my hearty thanks to Professor Mineo Kurokawa for the leadership and advices. I also thank all the co-authors for their continued support; T. Kitamura for Plat-E and Plat-A packaging cells; H. Nakauchi and M. Onodera for pGCDNsam-IRES-EGFP and KuOr retroviral vector; H. Miyoshi for constitutive and doxycycline-inducible lentiviral vector; A Miyawaki for phKO1 and Venus; F. Ueki, R. Toyama, and Y. Oikawa for expert technical assistance; van Lohuizen M and H. Koseki for Bmi1 knockout mouse; H. Wang for expression vectors.

References

1. Vardiman JW, Thiele J, Arber DA, et al. The 2008 revision of the World Health Organization (WHO) classification of myeloid neoplasms and acute leukemia: rationale and important changes. Blood. 2009;114:937-951.

2. Abdel-Wahab O, Mullally A, Hedvat C, et al. Genetic characterization of TET1, TET2, and TET3 alterations in myeloid malignancies. Blood. 2009;114:144-147.

3. Mardis ER, Ding L, Dooling DJ, et al. Recurring mutations found by sequencing an acute myeloid leukemia genome. N Engl J Med. 2009;361:1058-1066.

4. Boultwood J, Perry J, Pellagatti A, et al. Frequent mutation of the polycomb-associated gene ASXL1 in the myelodysplastic syndromes and in acute myeloid leukemia. Leukemia. 2010;24:1062-1065.

5. Chou WC, Huang HH, Hou HA, et al. Distinct clinical and biological features of de novo acute myeloid leukemia with additional sex comb-like 1 (ASXL1) mutations. Blood. 2010;116:4086-4094.

6. Yamashita Y, Yuan J, Suetake I, et al. Array-based genomic resequencing of human leukemia. Oncogene. 2010;29:3723-3731.

7. Ley TJ, Ding L, Walter MJ, et al. DNMT3A mutations in acute myeloid leukemia. N Engl J Med. 2010;363:2424-2433.

8. Yan XJ, Xu J, Gu ZH, et al. Exome sequencing identifies somatic mutations of DNA methyltransferase gene DNMT3A in acute monocytic leukemia. Nat Genet. 2011;43:309-315.

9. Thol F, Damm F, Ludeking A, et al. Incidence and prognostic influence of DNMT3A mutations in acute myeloid leukemia. J Clin Oncol. 2011;29:2889-2896.

10. Marcucci G, Metzeler KH, Schwind S, et al. Age-related prognostic impact of different types of DNMT3A mutations in adults with primary cytogenetically normal acute myeloid leukemia. J Clin Oncol. 2012;30:742-750.

11. Cancer Genome Atlas Research. Genomic and epigenomic landscapes of adult de novo acute myeloid leukemia. N Engl J Med. 2013;368:2059-2074.

12. Chen, T., Ueda, Y., Dodge, J. E., et al. Establishment and maintenance of genomic methylation patterns in mouse embryonic stem cells by Dnmt3a and Dnmt3b. Mol Cell Biol 2003;23, 5594-5605.

13. Holz-Schietinger C, Matje DM, Reich NO. Mutations in DNA methyltransferase (DNMT3A) observed in acute myeloid leukemia patients disrupt processive methylation. J Biol Chem. 2012;287:30941-30951.

14. Challen GA, Sun D, Jeong M, et al. Dnmt3a is essential for hematopoietic stem cell differentiation. Nat Genet. 2012;44:23-31.

15. Tadokoro Y, Ema H, Okano M, Li E, Nakauchi H. De novo DNA methyltransferase is essential for self-renewal, but not for differentiation, in hematopoietic stem cells. J Exp Med. 2007;204:715-722.

16. Simon JA, Kingston RE. Mechanisms of polycomb gene silencing: knowns and unknowns. Nat Rev Mol Cell Biol. 2009;10:697-708.

17. Kirmizis A, Bartley SM, Kuzmichev A, et al. Silencing of human polycomb target genes is associated with methylation of histone H3 Lys 27. Genes Dev. 2004;18:1592-1605.

18. Margueron R, Li G, Sarma K, et al. Ezh1 and Ezh2 maintain repressive chromatin through different mechanisms. Mol Cell. 2008;32:503-518.

19. Wang L, Brown JL, Cao R, Zhang Y, Kassis JA, Jones RS. Hierarchical recruitment of polycomb group silencing complexes. Mol Cell. 2004;14:637-646.

20. Morey L, Pascual G, Cozzuto L, et al. Nonoverlapping functions of the Polycomb group Cbx family of proteins in embryonic stem cells. Cell Stem Cell. 2012;10:47-62.

21. Villa R, Pasini D, Gutierrez A, et al. Role of the polycomb repressive complex 2 in acute promyelocytic leukemia. Cancer Cell. 2007;11:513-525.

22. Boukarabila H, Saurin AJ, Batsche E, et al. The PRC1 Polycomb group complex interacts with PLZF/RARA to mediate leukemic transformation. Genes Dev. 2009;23:1195-1206.

23. Neff T, Sinha AU, Kluk MJ, et al. Polycomb repressive complex 2 is required for MLL-AF9 leukemia. Proc Natl Acad Sci U S A. 2012;109:5028-5033.

24. Tanaka S, Miyagi S, Sashida G, et al. Ezh2 augments leukemogenicity by reinforcing differentiation blockage in acute myeloid leukemia. Blood. 2012;120:1107-1117.

25. Vire E, Brenner C, Deplus R, et al. The Polycomb group protein EZH2 directly controls DNA methylation. Nature. 2006;439:871-874.

26. Mohammad HP, Cai Y, McGarvey KM, et al. Polycomb CBX7 promotes initiation of heritable repression of genes frequently silenced with cancer-specific DNA hypermethylation. Cancer Res. 2009;69:6322-6330.

27. Chang Y, Sun L, Kokura K, et al. MPP8 mediates the interactions between DNA methyltransferase Dnmt3a and H3K9 methyltransferase GLP/G9a. Nat Commun. 2011;2:533.

28. Fuks F, Hurd PJ, Deplus R, Kouzarides T. The DNA methyltransferases associate with HP1 and the SUV39H1 histone methyltransferase. Nucleic Acids Res. 2003;31:2305-2312.

29. Zhao Q, Rank G, Tan YT, et al. PRMT5-mediated methylation of histone H4R3 recruits DNMT3A, coupling histone and DNA methylation in gene silencing. Nat Struct Mol Biol. 2009;16:304-311.

30. Widschwendter M, Fiegl H, Egle D, et al. Epigenetic stem cell signature in cancer. Nat Genet. 2007;39:157-158.

31. Ohm JE, McGarvey KM, Yu X, et al. A stem cell-like chromatin pattern may predispose tumor suppressor genes to DNA hypermethylation and heritable silencing. Nat Genet. 2007;39:237-242.

32. Schlesinger Y, Straussman R, Keshet I, et al. Polycomb-mediated methylation on Lys27 of histone H3 pre-marks genes for de novo methylation in cancer. Nat Genet. 2007;39:232-236.

33. Negishi M, Saraya A, Miyagi S, et al. Bmi1 cooperates with Dnmt1-associated protein 1 in gene silencing. Biochem Biophys Res Commun. 2007;353:992-998.

34. van der Lugt NM, Domen J, Linders K, et al. Posterior transformation, neurological abnormalities, and severe hematopoietic defects in mice with a targeted deletion of the bmi-1 proto-oncogene. Genes Dev. 1994;8:757-769.

35. Kumaki Y, Oda M, Okano M. QUMA: quantification tool for methylation analysis. Nucleic Acids Res. 2008;36:W170-175.

36. Habib M, Fares F, Bourgeois CA, et al. DNA global hypomethylation in EBV-transformed interphase nuclei. Exp Cell Res. 1999;249:46-53.

37. Tiacci E, Spanhol-Rosseto A, Martelli MP, et al. The NPM1 wild-type OCI-AML2 and the NPM1-mutated OCI-AML3 cell lines carry DNMT3A mutations. Leukemia. 2012;26:554-557.

38. Kallin, E. M., Cao, R., Jothi, R., Xia, K., Cui, K., Zhao, K., and Zhang, Y. (2009). Genome-wide uH2A localization analysis highlights Bmi1-dependent deposition of the mark at repressed genes. PLoS Genet 5, e1000506.

39. Gao Z, Zhang J, Bonasio R, et al. PCGF homologs, CBX proteins, and RYBP define functionally distinct PRC1 family complexes. Mol Cell. 2012;45:344-356.

40. Tavares L, Dimitrova E, Oxley D, et al. RYBP-PRC1 complexes mediate H2A ubiquitylation at polycomb target sites independently of PRC2 and H3K27me3. Cell. 2012;148:664-678.

41. Hollink IH, Feng Q, Danen-van Oorschot AA, et al. Low frequency of DNMT3A mutations in pediatric AML, and the identification of the OCI-AML3 cell line as an in vitro model. Leukemia. 2012;26:371-373.

42. Park IK, Qian D, Kiel M, et al. Bmi-1 is required for maintenance of adult self-renewing haematopoietic stem cells. Nature. 2003;423:302-305.

43. Iwama A, Oguro H, Negishi M, et al. Enhanced self-renewal of hematopoietic stem cells mediated by the polycomb gene product Bmi-1. Immunity. 2004;21:843-851.

44. Shen Y, Zhu YM, Fan X, et al. Gene mutation patterns and their prognostic impact in a cohort of 1185 patients with acute myeloid leukemia. Blood. 2011;118:5593-5603.

45. Kroon E, Krosl J, Thorsteinsdottir U, Baban S, Buchberg AM, Sauvageau G. Hoxa9 transforms primary bone marrow cells through specific collaboration with Meis1a but not Pbx1b. EMBO J. 1998;17:3714-3725.

46. Lin J, Yao DM, Qian J, et al. Recurrent DNMT3A R882 mutations in Chinese patients with acute myeloid leukemia and myelodysplastic syndrome. PLoS One. 2011;6:e26906.

47. Okano M, Bell DW, Haber DA, Li E. DNA methyltransferases Dnmt3a and Dnmt3b are essential for de novo methylation and mammalian development. Cell. 1999;99:247-257.

48. Hou HA, Kuo YY, Liu CY, et al. DNMT3A mutations in acute myeloid leukemia: stability during disease evolution and clinical implications. Blood. 2012;119:559-568.

49. Kronke J, Bullinger L, Teleanu V, et al. Clonal evolution in relapsed NPM1-mutated acute myeloid leukemia. Blood. 2013;122:100-108.

50. Wakita S, Yamaguchi H, Omori I, et al. Mutations of the epigenetics-modifying gene (DNMT3a, TET2, IDH1/2) at diagnosis may induce FLT3-ITD at relapse in de novo acute myeloid leukemia. Leukemia. 2013;27:1044-1052.

51. Busque L, Patel JP, Figueroa ME, et al. Recurrent somatic TET2 mutations in normal elderly individuals with clonal hematopoiesis. Nat Genet. 2012;44:1179-1181.

52. Yasuda T, Ueno T, Fukumura K, et al. Leukemic evolution of donor-derived cells harboring IDH2 and DNMT3A mutations after allogeneic stem cell transplantation. Leukemia. 2013.

53. Vassiliou GS, Cooper JL, Rad R, et al. Mutant nucleophosmin and cooperating pathways drive leukemia initiation and progression in mice. Nat Genet. 2011;43:470-475.

54. Antonchuk J, Sauvageau G, Humphries RK. HOXB4-induced expansion of adult hematopoietic stem cells ex vivo. Cell. 2002;109:39-45

55. Radulovic V, de Haan G, Klauke K. Polycomb-group proteins in hematopoietic stem cell regulation and hematopoietic neoplasms. Leukemia. 2013;27:523-533.

56. Sashida G, Iwama A. Epigenetic regulation of hematopoiesis. Int J Hematol. 2012;96:405-412.

57. Smith LL, Yeung J, Zeisig BB, et al. Functional crosstalk between Bmi1 and MLL/Hoxa9 axis in establishment of normal hematopoietic and leukemic stem cells. Cell Stem Cell. 2011;8:649-662.

58. Yuan J, Takeuchi M, Negishi M, Oguro H, Ichikawa H, Iwama A. Bmi1 is essential for leukemic reprogramming of myeloid progenitor cells. Leukemia. 2011;25:1335-1343.

59. Jacobs JJ, Scheijen B, Voncken JW, Kieboom K, Berns A, van Lohuizen M. Bmi-1 collaborates with c-Myc in tumorigenesis by inhibiting c-Myc-induced apoptosis via INK4a/ARF. Genes Dev. 1999;13:2678-2690.

60. Chowdhury M, Mihara K, Yasunaga S, Ohtaki M, Takihara Y, Kimura A. Expression of Polycomb-group (PcG) protein BMI-1 predicts prognosis in patients with acute myeloid leukemia. Leukemia. 2007;21:1116-1122.

61. Shih AH, Abdel-Wahab O, Patel JP, Levine RL. The role of mutations in epigenetic regulators in myeloid malignancies. Nat Rev Cancer. 2012;12:599-612.

62. Morey L, Aloia L, Cozzuto L, Benitah SA, Di Croce L. RYBP and Cbx7 define specific biological functions of polycomb complexes in mouse embryonic stem cells. Cell Rep. 2013;3:60-69.

63. Iwasaki H, Somoza C, Shigematsu H, et al. Distinctive and indispensable roles of PU.1 in maintenance of hematopoietic stem cells and their differentiation. Blood. 2005;106:1590-1600.

64. Mueller BU, Pabst T, Osato M, et al. Heterozygous PU.1 mutations are associated with acute myeloid leukemia. Blood. 2002;100:998-1007.

65. Vangala RK, Heiss-Neumann MS, Rangatia JS, et al. The myeloid master regulator transcription factor PU.1 is inactivated by AML1-ETO in t(8;21) myeloid leukemia. Blood. 2003;101:270-277.

66. Mizuki M, Schwable J, Steur C, et al. Suppression of myeloid transcription factors and induction of STAT response genes by AML-specific Flt3 mutations. Blood. 2003;101:3164-3173.

67. Heuser M, Argiropoulos B, Kuchenbauer F, et al. MN1 overexpression induces acute myeloid leukemia in mice and predicts ATRA resistance in patients with AML. Blood. 2007;110:1639-1647.

68. Mueller BU, Pabst T, Fos J, et al. ATRA resolves the differentiation block in t(15;17) acute myeloid leukemia by restoring PU.1 expression. Blood. 2006;107:3330-3338.

Tables

Table 1. A list of antibodies for flow cytometry

Epitope	Clone	Conjugate	Dilution	Company
Gr-1	RB6-8C5	Biotin	1:200	Bioleged
	RB6-8C5	APC	1:200	Bioleged
Mac-1	M1/70	Biotin	1:200	Bioleged
	M1/70	APC	1:200	Bioleged
B220	RA3-6B2	Biotin	1:200	Bioleged
	RA3-6B2	PerCP	1:200	BD
TER-119	TER-119	Biotin	1:200	Bioleged
CD3ε	145-2C11	Biotin	1:200	Bioleged
CD4	GK1.5	Biotin	1:200	Bioleged
CD8a	53-6.7	Biotin	1:200	Bioleged
CD127	A7R34	Biotin	1:200	Bioleged
Sca-1	E13-161.7	PerCP-Cy5.5	1:200	Bioleged
c-kit	2B8	APC	1:200	Bioleged
	2B8	PE-Cy7	1:200	BD
CD48	HM48-1	PE	1:200	BD
CD150	TC15-12F12.2	APC	1:200	Bioleged
F4/80	BM8	APC	1:200	Bioleged
CD11b (Human)	ICRF44	APC	1:200	Bioleged

Table 2. A list of PCR primer sequences

Gene	Species	Type	Forward	Reverse
PU.1	Mouse	BS sequencing	TTAGAGGGGATTGAGAAGAAAT	TCAAACCTACCCCCTAAACTAC
Hoxb2	Mouse	BS sequencing	AGAGGAGGAAGTTTTATGGTATTTAG	CAAATTCAAAATTCATAACTTTCAATA
PU.1 (URE)	Human	ChIP-qPCR	GCACACATGCTTCCTGTGGTGACT	CCACGTGCCCTGACTCCCCTCCTAGC
PU.1 (-5kb)	Human	ChIP-qPCR	ATCTGTTCACATGGGCTTCC	TGGTGGATAGGCAAGAAAGG
PU.1 (Proximal)	Human	ChIP-qPCR	CTGGTCAGCAGGAAATTGGT	GGGAACTGGGCAGTTGTTTA
Hoxa5	Mouse	RT-PCR	TATAGACGCACAAACGACCGC	CATTTGGATAGCGACCGCA
Hoxa9	Mouse	RT-PCR	GCGCCTTCTCCGAAAACA	CCGGGTTATTGGGATCGAT
Hoxb2	Mouse	RT-PCR	CCCGCTGTCTTGGAGACATTT	TTTTGGCTCCCTGGTCTCTGA
Hoxb4	Mouse	RT-PCR	TTCACTACAATCGCTACCTGACGC	GGTGTTGGGCAACTTGTGGTCTTT
Runx1	Mouse	RT-PCR	AACCCTCAGCCTCAAAGTCA	GGGTGCACAGAAGAGGTGAT
Nr4a2	Mouse	RT-PCR	CGCCGAAATCGTTGTCAGTA	CGACCTCTCCGGCCTTTTA
Foxo1	Mouse	RT-PCR	AAGAGGCTCACCCTGTCGC	GCATCCACCAAGAACTTTTCC
Meis1	Mouse	RT-PCR	CATGATAGACCAGTCCAACCGA	ATTGGCTGTCCATCAGGGTTA
Cebpα	Mouse	RT-PCR	AAACAACGCAACGTGGAGA	GCGGTCATTGTCACTGGTC
PU.1	Mouse	RT-PCR	CAGAAGGGCAACCGCAAGAA	GCCGCTGAACTGGTAGGTGA
Gata3	Mouse	RT-PCR	GGGTTCGGATGTAAGTCGAG	CCACAGTGGGGTAGAGGTTG
Pbx1	Mouse	RT-PCR	AGGACATCGGGGACATTTTAC	CATTAAACAAGGCAGGCTTCA
Evi1	Mouse	RT-PCR	GGAGGAGGACTTGCAACAAA	GACAGCATGTGCTTCTCCAA
Mef2c	Mouse	RT-PCR	AGGTGTTGCTCAAGTACACCGAGT	ATCTCAAAGCTGGGAGGTGGAACA
PU.1	Human	RT-PCR	GGGAGAGCCATAGCGACCAT	TAGGAGACCTGGTGGCCAAGA
18s rRNA	Human Mouse	RT-PCR	GTAACCCGTTGAACCCCATT	CCATCCAATCGGTAGTAGCG